ICT-619555 RESCUE

D2.2.1 Version 1.0

Interim Report of Detailed Optimisation Algorithm and Performance Comparisons

Contractual Date of Delivery to the CEC:	04/2015 (M18)
Actual Date of Delivery to the CEC:	04/2015
Editor:	Jiancao Hou
Authors:	Tad Matsumoto, Shen Qian, Jiancao Hou, Na Yi, Maximilian Matthé, Albrecht Wolf, Valtteri Tervo, Xiaobo Zhou
Participants:	JAIST, UNIS, TUD, UOULU
Work package:	WP2 – Code and algorithm design and optimization
Security:	**PU**
Nature:	**R**
Version:	1.0
Total number of pages:	49

Abstract: One of the main tasks of RESCUE project is to exploit the optimal power allocation of the transmission nodes in the network to improve the system performance. In this deliverable, the intermediate results on the physical layer power optimisation algorithms with respect to different toy scenarios described in D1.2.1 are provided. Start from the toy scenario one, the outage probability based power allocation for the basic lossy-forward relaying system is investigated. Moreover, the system model is extended to multi-antenna case, where the relay-oriented source power allocation for the erroneous decode-and-forward relaying system is provided. For the toy scenario two, apart from the outage probability based power allocation, the joint relay nodes power allocation to equalize the signal to noise ratios limits for each relay decoder is also considered. Furthermore, the optimal power allocation algorithm for orthogonal multiple access relay channel with intra-link errors is proposed. Simulation results are provided to illustrate the improved performance of all the proposed algorithms by comparing with the conventional schemes.

Keyword list: power allocation, relay channel, erroneous decode-and-forward, outage probability, multiple antennas, chief executive officer, multiple access

Executive Summary

The integrated concept "links-on-the-fly" of the RESCUE project allows relays decode-and-forward (DF) data symbols with specified level of loss/distortion, which aims to create efficient and robust information transfer through multi-path networks. In this case, the optimal power allocation on each link/node can significantly enhance the efficiency and robustness of the network and keep the rate distortion below a certain specified limit. In order to present the merit of power allocation strategy in the RESCUE project, in this interim report, some detailed power optimization algorithms are evaluated using different toy scenarios provided in D1.2.1.

For the toy scenario one (TS1), the theoretical outage bound of the lossy-forwarding system is derived over block Rayleigh fading channels and the existing results are just obtained by numerical computations for multi-fold integrals with equal power allocation at each transmitter. By assuming high SNR values, the closed-form expression of the outage probability can be mathematically derived. Thus, the optimal power allocation in order to minimize the outage probability subject to the total power constraint can be formulated as convex optimization problem and solved by using a convex optimization tool. Moreover, without the global channel knowledge to be assumed at each node, the conventional multi-antenna based erroneous DF relaying network normally allows the source optimize its transmit power on its direct channel links to its served users. Meanwhile, the relay node comes to help if its received signal to interference plus noise ratios of certain data streams can pass the predetermined threshold. However, such strategy may loss the system performance if the source node has the location and power budget information of the relay node. This motivates the relay oriented source power allocation algorithm to be proposed to improve the system performance.

The toy scenario two (TS2) assume that multiple relays are deployed to help the information transmission from the source node to the destination node. Without the direct link between the source node and the destination node (i.e., S-D link) and all the source node to relay node links (i.e., S-R links) are lossy, the system is known as the chief executive officer (CEO) problem. As the way of analysing TS1, the outage probability based power allocation algorithm for CEO problem is also investigated. Moreover, according to the theoretical analysis, the relation between bit flipping probabilities and mutual information values can be built, where any relay decoder with low bit flipping probability benefits to a greater extent from the high mutual information. Here, the bit flipping probabilities can be controlled by the power allocation on the relay nodes. Hence, with the proposed joint relay nodes power allocation algorithm, the signal to noise ratios limits for each relay decoder can be equalized, such that the ramp region of the joint decoder can be removed or reduced.

As mentioned in D1.2.1, the toy scenario three (TS3) is an extension of TS1, and it can be deemed as combining multiple independent TS1 together. In this case, based on the different channel conditions of S-R links, the power allocation algorithms proposed for TS1 can be used to solve TS3 problem via proportionally splitting the total transmit power for each relay node. Moreover, TS3 can be composed by the TS2 plus the S-D link, therefore additional information can be involved in the decoding process to further improve the system performance.

Consider the toy scenario four (TS4), where the orthogonal multiple access relay channel allows that the intra-link errors exist. It has been found that even the relay node cannot correctly decode the estimates, at the destination node, the forwarded erroneous estimates are still helpful for the reconstruction of the information sequence sent from the source nodes. Moreover, by forwarding the specific level of incorrectly decoded estimates, the system outage performance can be improved especially when one of the source nodes is quite far away from both the relay node and the destination node. Under such circumstances, the optimal power allocation among the source nodes and the relay node subject to lossy rate constraints is exploited. The system performance is improved by comparing with traditional DF in terms of total power consumption especially in the cases where the relay node is close to the destination node.

To sum up, the above described power allocation algorithms for different toy scenarios are only the intermediate research results of the RESCUE project, where the detailed algorithm description and comparison have been included in this deliverable. More comprehensive analytical results and computer simulation of all the proposed power optimization algorithms will be carried out in the final report.

Authors

Partner	Name	E-mail / Phone
Japan Advanced Institute of Science and Technology (JAIST)	Tad Matsumoto Shen Qian	matumoto@jaist.ac.jp shen.qian@jaist.ac.jp
University of Surrey (UNIS)	Jiancao Hou Na Yi	j.hou@surrey.ac.uk/+44 1483 682229 n.yi@surrey.ac.uk
Technical University Dresden (TUD)	Maximilian Matthé Albrecht Wolf	maximilian.matthe@tu-dresden.de albrecht.wolf@tu-dresden.de
University of Oulu (UOULU)	Valtteri Tervo Xiaobo Zhou	valtteri.tervo@ee.oulu.fi xiaobo.zhou@ee.oulu.fi

Table of Contents

List of Acronyms and Abbreviations

Term	Description
AWGN	Additive White Gaussian Noise
BCJR	Bahl Cocke Jelinek Raviv
BER	Bit Error Rate
BSC	Binary Symmetric Channel
CCC	Constellation Constrained Capacity
CEO	Chief Executive Officer
CPU	Central Processing Unit
CSI	Channel State Information
DF	Decode-and-Forward
EP	Equal Power
FDD	Frequency-Division Duplex
i.i.d.	Independent and Identically Distributed
JD	Joint Decoder
KPI	Key Performance Indicator
LOS	Line of Sight
LosFoR	Lossy-Forwarding Relay
MARC	Multiple Access Relay Channel
MIMO	Multiple Input Multiple Output
OFDMA	Orthogonal Frequency Division Multiple Access
OPA	Optimal Power Allocation
PDF	Probability Density Function
R-D	Relay-Destination
RF	Rayleigh Fading
RESCUE	Links-on-the-fly Technology for Robust, Efficient, and Smart Communication in Unpredictable Environments
SCA	Successive Convex Approximation
SCS	Source-Channel Separation
S-DF	Selective Decode-and-Forward
SDR	Software Defined Radio
SINR	Signal-to-Interference-plus-Noise Ratio
SNR	Signal-to-Noise Ratio
S-D	Source-Destination
S-R	Source-Relay
TDD	Time-Division Duplex
TS	Toy Scenario
WSN	Wireless Sensor Network
WSRM	Weighted Sum Rate Maximization
ZF	Zero-Forcing

1. Introduction

In conventional communication systems, accurate/strict link-budget allocation, strong error-correction coding and retransmission protocols are needed to keep the communications with high transmission rate and the outage probability in an acceptable range. However, such kind of system design sacrifices the energy/spectral efficiencies due to the sophisticated decoding and channel estimation techniques plus a large amount of signalling overhead. Moreover, it performs poorly or completely fail the communications if the transmission environment is unpredictable, such as in the presence of earthquakes or tsunamis. These motivated the RESCUE project to develop robust, efficient, and smart communication systems by using the concept "links-on-the-fly".

The basic idea of "links-on-the-fly" is to allow the specified level of erroneously decoded data streams at the relay node to be forwarded to the destination node. Thus, the required power to be allocated to each link can be significantly reduced in the network as a whole. Moreover, such decoding errors can be estimated at the destination node through the proposed decoding techniques which were introduced in D2.1.1. Here, apart from the decoding techniques, another major physical layer research task is the transmit power optimization under various constraints. In detail, the optimization issues can be mainly categorized into two parts: One is the total transmit power of all nodes minimization subject to the fixed distortion or rate constraints; The other is the distortion minimization or the rate maximization subject to the total power constraint. As we can see, the two objectives are dual to each other, and the tools from joint convex and combinatorial optimization theory can be used to solve the problems. In this case, proposing the complexity-reduced power optimization algorithms plays a major role of enhancing the energy efficiency of the system.

As discussed in D1.2.1, the theoretical analysis and performance evaluation of the RESCUE network model presents a lot of challenges due to its complicated and dynamic network topology. Instead, we decompose the general network into four basic toy scenarios in order to facilitate our analysis. Such strategy is also applied to the power optimization algorithms design in this deliverable, and this motivated us to categorize the work based on different toy scenarios (TSs):

TS1 Firstly, a sufficiently accurate closed-form expression of the outage probability is derived by taking the geometrical gain into account, and the optimal power allocation scheme can be formulated to the convex problem for minimizing the outage probability while keeping the total transmit power constraint or minimizing the transmit power while keeping the outage probability fixed. Then, we extend the system model to the multiple input multiple output (MIMO) case to exploit the multiplexing gain. Without the channel knowledge of relay-destination (R-D) link at the source node, the conventional relaying strategy allocates the source's power based on the source-destination (S-D) link, and the system performance is not enhanced if the source node has the location power budget information of the relay node. This motivated the relay-oriented source power allocation algorithm to be proposed to improve the system performance.

TS2 According to the "Slepian-Wolf Admissible Rate Region based Outage Probability Derivation for CEO" of deliverable D1.2.1, the approximated closed-form expression of the outage probability for high signal to noise ratio (SNR) of the system model is provided, and the optimal power allocation scheme can also be formulated as a convex problem for minimizing the outage probability while keeping the total transmit power constraint or minimizing the transmit power while keeping the outage probability fixed. Then, we investigate a power allocation algorithm to equalize the SNR limits for each relay decoder, such that the ramp region of the joint decoder at the destination node can be removed or reduced. Here, the SNR limit is defined as the bit error rate (BER) curve reaches its error floor for each relay decoder.

TS3 As we explained in D1.2.1, TS3 is an extension of TS1, where multiple relays coexist in the system to help the information transmission from the source node to the destination node. In this case, following the "links-on-the-fly" concept, different relay nodes can base on their different source-relay (S-R) links statistic properties to do the power allocation. In other words, TS3 can be divided into several independent and parallel TS1s, and by given the total transmit power budget, we can propositionally allocate the power to the different transmission nodes. According to the above discussion, the power allocation strategies for TS3 can be refer to the power allocation strategies for TS1.

TS4 Consider the orthogonal multiple access relay channel (MARC), where two source nodes are communicating with a common destination node with the assist of a relay node. Comparing with the conventional

decode-and-forward (DF) relaying strategies, it has been shown in the literature that even the estimates are incorrectly decoded at the relay node, the forwarded erroneous estimates are still helpful for the destination node to reconstruct the information sequences sent from the source nodes. This motivates us to investigate the power minimization problem subject to lossy rate constraints for MARC by comparing with the lossless DF. Such a problem has been deemed as a non-convex problem, and the successive convex approximation (SCA) algorithm can be implemented to solve it.

In addition, in order to evaluate the performance of the proposed power allocation algorithms which are mentioned above, apart from the physical-layer computer simulations, implementing the algorithms to the small-scale software defined radio (SDR) platform (e.g., 4 USRP2 boards) is also very important, where the interaction with WP3 is required. In detail, we have agreed to produce some interfaces of the algorithms, and then the blackbox based simulation can be built up to link the proposed power algorithms with the SDR devices. In this case, one of the key steps is to provide the channel requirements for each proposed algorithm. For example, for outage probability minimization problem, the statistical characterization of the channels is only needed to optimally allocate the power, where the statistical channel information can be obtained through the long-term observation for either time-division duplex (TDD) or frequency-division duplex (FDD) models. Or, considering to solve the chief executive officer (CEO) problem, the bit flipping probabilities is only needed for the joint relay nodes power allocation, where such kind of information can be linked with some quantized information, e.g., the SNRs at the relay node, and stored at the predetermined look-up table.

It is worthwhile to note that, in this deliverable, we also produce some power allocation algorithms which need the instantaneous local or global channel knowledge at each node. Such algorithms requires a central processing unit (CPU) to collect the information, perform the processing and report the allocated powers back to each transmission nodes. Although the algorithms with instantaneous channel are not quite practical to be implemented, they can be good baselines for us to further investigate the power allocation algorithms of the erroneous DF based relaying network.

2. Power Allocation for Basic Erroneous Decode-and-Forward Relaying Network

2.1 Outage Based Power Allocation for a Lossy-Forwarding Relaying System

2.1.1 Motivation and Objective

In [AM12], a novel lossy-forwarding relay (LosFoR) system allowing erroneous information to be transmitted by the relay is proposed. The information sequence, obtained as the result of relay decoding, is interleaved, re-encoded and transmitted to the destination, even it includes errors occurring in the S-R transmission (lossy-forwarding). At the destination, the S-R link error probability is estimated, and used as a correlation knowledge between the information sent from source and relay. The theoretical outage bound of the LosFoR system is derived over block Rayleigh fading channels [ZCH+14], which assumes that the bit error probability after decoding at the relay is a random variable which changes according to the S-R variation. By imposing Shannon's lossy source-channel separation (SCS) theorem, the relationship between the S-R channel error probability and its corresponding instantaneous SNR is established. However, only equal power allocation is adopted for each transmitter (at both S and R) in [ZCH+14], and the results are just obtained by numerical computations for multi-fold integrals. Moreover, another important performance metric − geometrical gain, which is very important for protocol design − has not been related to power allocation analysis of the LosFoR scheme.

The major purpose of this section is to analyse the optimum power allocation of the LosFoR system in more practical scenarios, where all channels experience fading variation. By assuming high SNR values for such a system scenario, closed-form expression of the outage probability is mathematically derived. It is shown that the power allocation for the proposed LosFoR system can be formulated as a convex optimization problem. The optimum power allocation scheme for minimizing the outage probability is then presented, where geometrical gain is taken into account. We found that proposed optimal power allocation scheme improve outage performance compared with the equal power allocation, when R is located close to D. Also, this section investigates the impact of line-of-sight (LOS) component on optimum power allocation of the LosFoR system.

2.1.2 System Model

In this section, a very simple three-node relay transmission model is considered, as shown in Fig. 2.1. During the first time slot, the original information sequence $\mathbf{b}_1$ is broadcasted from the S to both R and D. As in the DF scheme, the original information sequence is decoded and re-constructed at R, before being forwarded as $\mathbf{b}_2$. In contrast to the conventional DF system, our proposed technique always interleaves the re-constructed sequence at R, and then re-encodes and maps it for the second time slot transmission. It should be noted that the re-constructed bit sequence may contain some errors, due to the imperfectness transmission of S-R channel, but it is still highly correlated with the original one sent from S.

After receiving signals from both S and R, joint decoding process takes place at D. It is already known that by exploiting the correlation knowledge between the bit sequences sent from S and R, the minimum rate required for lossless transmission is no longer equal to the entropy of each source, but could be even lower, as stated by the

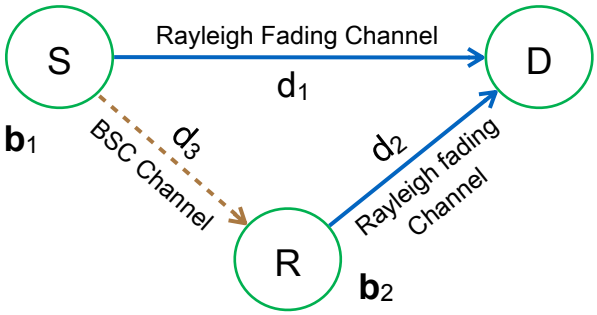

Figure 2.1: Single relay transmission system.

Slepian-Wolf theorem. In other words, if we keep transmitting the redundancy (the correlated portion), the whole system performance will benefit from utilizing the correlation knowledge.

All the three transmission channels are assumed to suffer from independent block fading. Hence, it is reasonable to use the binary symmetric channel (BSC) model [GZ05], with the crossover probability p_e as a parameter within one block. Hence, $\mathbf{b}_2 = \mathbf{b}_1 \oplus \mathbf{e}$, where $\oplus$ denotes modulo-2 addition and $\mathbf{e}$ is a binary error vector. $\Pr(e = 1) = p_e$ is fixed within each block, and the p_e value changes block-by-block. $p_e = 0$ indicates the perfect decoding at R, while $p_e \neq 0$ indicates there exist S-R link errors which could not be eliminated by the decoding process at R.

In this section, all the links are assumed to be suffering from block Rayleigh fading whose probability density function (PDF) with instantaneous SNR γ_i is given by

$$p(\gamma_i) = \frac{1}{\Gamma_i} \exp(-\frac{\gamma_i}{\Gamma_i}), (i = 1,2,3), \tag{2.1}$$

where Γ_i represent received average SNRs of the S-D, R-D and S-R channels, respectively.

With d_i (i=1,2,3) representing the length of S-D, R-D and S-R channels, respectively. With the geometrical gain of the S-D channel, G_1, being normalized to one, the geometric gains of R-D and S-R channels, G_2 and G_3, can be defined as [LNH10]

$$\begin{aligned} G_2 &= \left(\frac{d_1}{d_2}\right)^{\alpha}, \\ G_3 &= \left(\frac{d_1}{d_3}\right)^{\alpha}, \end{aligned} \tag{2.2}$$

where the path-loss factor α is set to 3.52 [YG11]. For sake of simplicity, the variation due to shadowing is ignored in this section.

2.1.3 Outage Probability Derivation

Based on Shannon's lossy SCS theorem, for S-R channel, we have $R_3(\mathscr{D})R_{c3} \leqslant C(\gamma_3)$, where $R_3(\mathscr{D})$ is the rate function of distortion D with $\mathscr{D} = p_e$, R_{c3} denotes the spectrum efficiency including the channel coding scheme and the modulation multiplicity and $C(\gamma_3)$ is the capacity with instantaneous SNR γ_3 of S-R channel. For hamming distortion measure, $R_3(\mathscr{D}) = 1 - H(\mathscr{D})$.

With the relationship between p_e and γ_3, the rate constrains supported by the Slepian-Wolf theorem are given by [ZCH+14]

$$\begin{aligned} R_1 &\geqslant H(\mathbf{b}_1 \mid \mathbf{b}_2), \\ R_2 &\geqslant H(\mathbf{b}_2 \mid \mathbf{b}_1), \\ R_1 + R_2 &\geqslant H(\mathbf{b}_1, \mathbf{b}_2) = 1 + H(p_e) = 1 + H\left[R_3^{-1}\left(\frac{C(\gamma_3)}{R_{c3}}\right)\right], \end{aligned} \tag{2.3}$$

where R_1 and R_2 are source rate for $\mathbf{b}_1$ and $\mathbf{b}_2$, respectively. $H(\cdot|\cdot)$ and $H(\cdot,\cdot)$ denote the conditional entropy and the joint entropy between the arguments, respectively.

Actually, the Slepian-Wolf theorem, which intends to recover two correlated sources, is not perfectly suitable for the system setup in this section since the destination only aims to reconstruct the information sent from S. However, the difference between exact outage derived from theorem for source coding with side information and the approximation outage derived from Slepian-Wolf theorem is negligible [ZCH+14]. For simplicity reason on calculation, in this section, the outage probability is calculated based on Slepian-Wolf theorem.

Eq. (2.3) can be understood from the viewpoint of the Slepian-Wolf rate region presented in Fig. 2.2 and Fig. 2.3. According to the value of $R_3(\mathscr{D})$, the rate constrains can be divided into two cases for discussing:

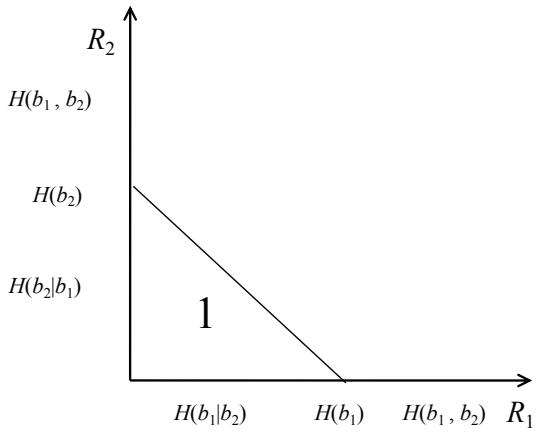

Figure 2.2: Lossy transmission of the S-R channel, $0 < p_e \leqslant 0.5$.

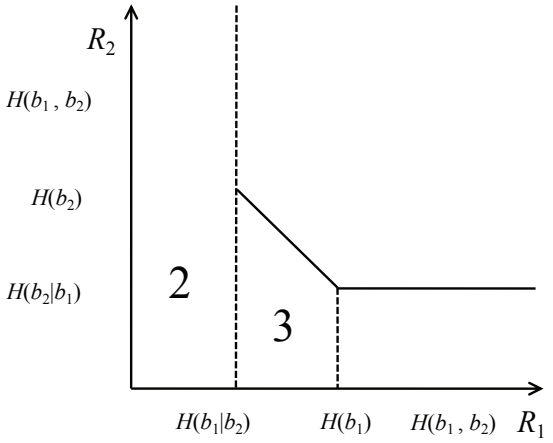

Figure 2.3: Slepian-Wolf rate regions of the proposed relay system.

1. $R_3(\mathscr{D}) \geq 1$ ($p_e = 0$), implying that perfect decoding is conducted at R. In this case, the outage event happens when R_1 and R_2 are within Area 1 shown in Fig. 2.2. The probability which R_1 and R_2 fall into Area 1 is denoted as P_1;

2. $0 \leqslant R_3(\mathscr{D}) < 1$ ($0 < p_e \leqslant 0.5$), indicating that decoding at the relay is imperfect. S-R channel SNR cannot support error-free transmission. Then, the outage event occurs when R_1 and R_2 are inside Areas 2 and 3 shown in Fig. 2.3, which the probabilities are denoted by P_2 and P_3, respectively. Hence, the total outage probability of the LosFoR system can be defined by

$$P_{out} = P_1 + P_2 + P_3. \tag{2.4}$$

It is found that the outage probability can be calculated by using a triple integral with respect to the joint pdf of the instantaneous SNRs $p(\gamma_1, \gamma_2, \gamma_3)$ [ZCH+14], given the range defined in (2.3). Since we assume that the variation of each link's instantaneous SNR is statistically independent,

$$p(\gamma_1, \gamma_2, \gamma_3) = p(\gamma_1)p(\gamma_2)p(\gamma_3). \tag{2.5}$$

With the assumption that Gaussian codebook is used, the relationship between the instantaneous channel SNR γ_i

and its corresponding source rate R_i is given by

$$R_i \leq \frac{E^n}{2R_{ci}} \log_2 \left(1 + \frac{2\gamma_i}{E^n}\right), (i = 1,2,3) \tag{2.6}$$

where E^n denotes the signalling dimensionality. In this section, we assume $E^n = 2$. R_{ci} denotes the system efficiency of the transmission chain representing the coding rate and multiplicity of the modulation for *i-th* (i = 1, 2, 3) channel.

In practical systems, the channel capacity is upper bounded by the multiplicity of modulation. However, the difference between the constellation constrained capacity (CCC) and Gaussian capacity is very small in low SNR region. While in high SNR region, distortion level $\mathscr{D}$ is very close to 0, resulting in $p_e = 0$. The difference between CCC and Gaussian capacity does not have any significant impact on $\mathscr{D}$ for the entire SNR region. Therefore, it is reasonable to replace CCC by Gaussian capacity for outage derivation.

By converting the rate constrains into the instantaneous SNR constrains [CAM13b], the theoretical calculation of the outage probability P_1, P_2 and P_3 can then be mathematically expressed as,

$$\begin{aligned} P_1 =& \Pr[0 < R_1 < H(\mathbf{b}_1), 0 < R_2 < H(\mathbf{b}_1, \mathbf{b}_2), R_3 \geq 1] \\ =& \int_{\gamma_1=0}^{1} \int_{\gamma_2=0}^{2^{1-\log_2(1+\gamma_1)}-1} \int_{\gamma_3=1}^{\infty} p(\gamma_1)p(\gamma_2)p(\gamma_3)d\gamma_1 d\gamma_2 d\gamma_3 \\ =& \frac{1}{\Gamma_1} \exp\left(-\frac{1}{\Gamma_3}\right) \int_{1}^{\gamma_1=0} \exp\left(-\frac{\gamma_1}{\Gamma_1}\right) \cdot \left[1 - \exp\left(-\frac{2^{1-\log_2(1+\gamma_1))} - 1}{\Gamma_2}\right)\right] d\gamma_1, \end{aligned} \tag{2.7}$$

$$\begin{aligned} P_2 =& \Pr[0 < R_1 < H(\mathbf{b}_1 \mid \mathbf{b}_2), R_2 > 0, 0 \leq R_3 < 1] \\ =& \int_{\gamma_1=0}^{2^{H(pe)}-1} \int_{\gamma_2=0}^{\infty} \int_{\gamma_3=0}^{1} p(\gamma_1)p(\gamma_2)p(\gamma_3)d\gamma_1 d\gamma_2 d\gamma_3 \\ =& \frac{1}{\Gamma_3} \int_{\gamma_3=0}^{1} \exp\left(-\frac{\gamma_3}{\Gamma_3}\right) \cdot \left[1 - \exp\left(-\frac{2^{1-\log_2(1+\gamma_3)} - 1}{\Gamma_1}\right)\right] d\gamma_3, \end{aligned} \tag{2.8}$$

$$\begin{aligned} P_3 =& \Pr[H(\mathbf{b}_1 \mid \mathbf{b}_2) < R_1 < H(\mathbf{b}_1), 0 < R_2 < H(\mathbf{b}_1, \mathbf{b}_2) - R_1, 0 \leq R_3 < 1] \\ =& \int_{\gamma_1=2^{H(pe)}-1}^{1} \int_{\gamma_2=0}^{2^{1+H(pe)-\log_2(1+\gamma_1)}-1} \\ & \int_{\gamma_3=0}^{1} p(\gamma_1)p(\gamma_2)p(\gamma_3)d\gamma_1 d\gamma_2 d\gamma_3, \\ =& \frac{1}{\Gamma_1}\frac{1}{\Gamma_3} \int_{\gamma_1=2^{1-\log_2(1+\gamma_3)-1}}^{1} \int_{\gamma_3=0}^{1} \exp\left(-\frac{\gamma_1}{\Gamma_1}\right) \exp\left(-\frac{\gamma_3}{\Gamma_3}\right) \cdot \left[1 - \exp\left(-\frac{2^{2-\log_2(1+\gamma_3)-\log_2(1+\gamma_1)} - 1}{\Gamma_2}\right)\right] d\gamma_1 d\gamma_3. \end{aligned} \tag{2.9}$$

The values of P_1, P_2 and P_3 can be calculated by numerical method [Sha08], with sufficiently accurate numerical calculation error control.

2.1.4 Optimal Power Allocation

The goal of this section is to minimize the outage probability while the total transmit power E_T is fixed, and to minimize E_T while keeping the outage probability constant. The noise variance ${\sigma_n}^2$ of each channel is normalized to unity. The transmit powers, which are now equivalent to their corresponding average SNRs, allocated to S and R are denoted as kE_T and $(1-k)E_T$, respectively, where k ($0 < k < 1$) is power allocation ratio.

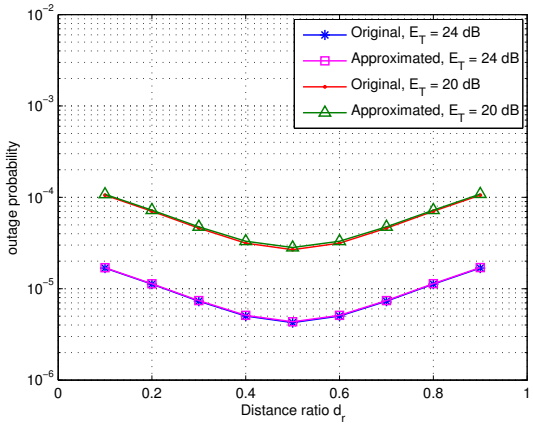

Figure 2.4: Accuracy of the approximated closed-form outage expression.

While keeping the ratio k constant and bringing the average SNRs Γ_1, Γ_2 and Γ_3 to infinity, by invoking the property of exponential function $e^{-x} \approx 1-x$ for small x, at the high SNR regime, the outage probability (2.4) can be approximated to a closed-form expression, as,

$$P_{out} \approx \frac{0.5}{E_T^2 k^2 G_1^2} + \frac{0.5}{E_T^2 k^2 G_3^2} + \frac{1.3863}{E_T^2 k^2 G_1 G_3} + \frac{0.3863}{E_T^2 k(1-k) G_1 G_2}. \tag{2.10}$$

To identify the accuracy of the approximation, outage probability curves obtained by using the approximated expression (2.10), and by numerically calculating (2.7)-(2.9), are presented in Figure 2.4. The relay node is assumed to be allocated in the line between the source and the destination, and the distance ratio is defined by $d_r = d_2/d_1$. Good matching is illustrated between the curves of approximation and numerical calculation, which indicates sufficient accuracy of the approximation. Then, the optimal power allocation problem is formulated by a standard optimization problem, which can be proven to be convex.

2.1.4.1 Proof of Convexity

Here we give the proof of the convexity of the approximated outage probability expression, Eq. (2.10), with regard to variables E_T and k. If each of the four terms in Eq. (2.10) can be proven to be convex, (2.10) is also convex because it is a sum of the convex terms. The Hessian matrix of the first term $\frac{0.5}{E_T^2 k^2 G_1^2}$ can be calculated as

$$\mathbf{H}\left[\frac{0.5}{E_T^2 k^2 G_1^2}\right] = \frac{1}{E_T^2 G_1^2 k^2}\begin{bmatrix} \frac{3}{k^2} & \frac{2}{E_T k} \\ \frac{2}{E_T k} & \frac{3}{E_T^2} \end{bmatrix}. \tag{2.11}$$

The eigenvalues of (2.11)

$$\lambda_{1,2} = \frac{1}{2E_T^2 G_1^2 k^2}\left(\frac{3}{k^2} + \frac{3}{E_T^2} \pm \sqrt{\left(\frac{3}{k^2} + \frac{3}{E_T^2}\right)^2 - \frac{20}{E_T^2 k^2}}\right) \tag{2.12}$$

are clearly non-negative. Therefore, the Hessian matrix of $\frac{0.5}{E_T^2 k^2 G_1^2}$ is positive semi-definite and hence its convexity has been proven.

The Hessian matrix of the second term $\frac{0.5}{E_T^2 k^2 G_3^2}$ can be calculated as

$$\mathbf{H}\left[\frac{0.5}{E_T^2 k^2 G_3^2}\right] = \frac{1}{E_T^2 G_3^2 k^2}\begin{bmatrix} \frac{3}{k^2} & \frac{2}{E_T k} \\ \frac{2}{E_T k} & \frac{3}{E_T^2} \end{bmatrix}. \tag{2.13}$$

The eigenvalues of (2.13)

$$\lambda_{1,2} = \frac{1}{2E_T^2 G_1^2 k^2}\left(\frac{3}{k^2}+\frac{3}{E_T^2} \pm \sqrt{\left(\frac{3}{k^2}+\frac{3}{E_T^2}\right)^2 - \frac{20}{E_T^2 k^2}}\right) \tag{2.14}$$

are clearly non-negative. Therefore, the Hessian matrix of $\frac{0.5}{E_T^2 k^2 G_3^2}$ is also positive semi-definite and hence its convexity has been proven.

Similarly, the Hessian matrix of the third term $\frac{1.3863}{E_T^2 k^2 G_3 G_1}$ can be calculated as

$$\mathbf{H}\left[\frac{1.3863}{E_T^2 k^2 G_3 G_1}\right] = \frac{1}{E_T^2 G_3 G_1 k^2}\begin{bmatrix} \frac{8.3178}{k^2} & \frac{5.5452}{E_T k} \\ \frac{5.5452}{E_T k} & \frac{8.3178}{E_T^2} \end{bmatrix}. \tag{2.15}$$

The eigenvalues of (2.15)

$$\lambda_{1,2} = \frac{1}{2}\left(\frac{8.3178}{k^2}+\frac{8.3178}{E_T^2} \pm \sqrt{\left(\frac{8.3178}{k^2}+\frac{8.3178}{E_T^2}\right)^2 - \frac{153.7468}{E_T^2 k^2}}\right) \tag{2.16}$$

are clearly non-negative. Therefore, the Hessian matrix of $\frac{1.3863}{E_T^2 k^2 G_3 G_1}$ is positive semi-definite and hence its convexity has been proven.

The Hessian matrix of the fourth term $\frac{0.3863}{E_T^2 k(1-k) G_1 G_2}$ can be calculated as

$$\mathbf{H}\left[\frac{0.7726}{E_T^2 k(1-k) G_1 G_2}\right] = \frac{1}{k^3(1-k)^3 E_T^4 G_1 G_2}\cdot\begin{bmatrix} E_T^2(3k^2-3k+1) & E_T k(2k^2-3k+1) \\ -E_T k(2k^2-3k+1) & 3k^2(k^2-2k+1) \end{bmatrix}. \tag{2.17}$$

Let $u(k) = 3k^3(k^2-2k+1) + E_T^2(3k^2-2k+1)$ and $v(k) = 3k^2E_T^2(3k^3-3k+1)(k^2-2k+1)$, the eigenvalues of (2.17) can be calculated as

$$\lambda_{1,2} = \frac{u(k) \pm \sqrt{u(k)^2 - 4v(k)}}{2}. \tag{2.18}$$

For $0 < k < 1$, the value of the quadratic polynomials k^2-2k+1 and $3k^2-2k+1$ in $u(k)$, and the quadratic polynomials $3k^3-3k+1$ and k^2-2k+1 in $v(k)$ are larger than 0. This indicates the non-negativity of $u(k)$ and $v(k)$. Hence, the Hessian matrix of $\frac{0.3863}{E_T^2 k(1-k) G_1 G_2}$ is proven to be positive semi-definite and hence its convexity has been proven. Therefore, the outage probability expression (2.10) is a convex function.

2.1.4.2 Optimal Power Allocation: Total Power Fixed

In this subsection, we minimize the outage probability while the total power E_T is fixed. The convex problem can be formulated as

$$\begin{array}{ll} \underset{k}{\text{minimize}} & P_{out}(k, E_{\mathrm{T}}) \\ \text{subject to} & k-1<0 \\ & -k<0. \end{array} \tag{2.19}$$

The solution to the optimization problem can be obtained by using a convex optimization tool, and optimal values of k are listed in Table 2.1. Obviously, the larger the d_r value, the more transmit power should be allocated to S.

Theoretical results for the outage performance with and without optimal power allocation are shown in Fig. 2.5, where the total transmit power E_T is set at 16 dB. First of all, it can be obviously seen that with equal power allocation, the outage curve is symmetric to the mid-point between S and D, which yields the lowest outage

Table 2.1: Optimal power ratio k

d_r	optimal k ($E_T = 16$ dB)
0.1	0.500
0.2	0.502
0.3	0.520
0.4	0.574
0.5	0.666
0.6	0.774
0.7	0.871
0.8	0.943
0.9	0.985

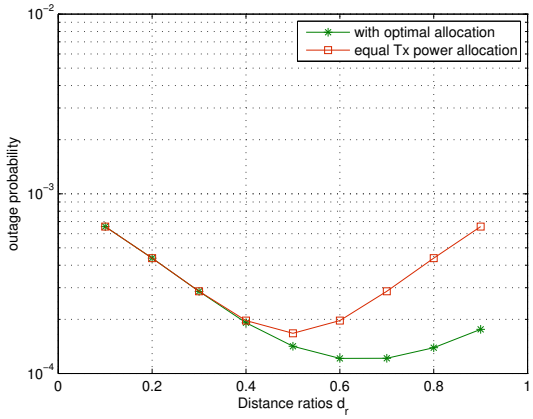

Figure 2.5: Outage probabilities with and without optimal power allocation, total transmit power fixed.

probability. This finding is different from the conventional DF case, of which R should be located at a point closer to S in order to achieve the best performance [ZCH+14]. The optimal power allocation provides the lowest outage probability at the point where the contributions of both S-R and R-D channels to outage are balanced. In other words, the proposed technique enables the transmitter to find proper relays for cooperation in a broader area. It should be noted that, by selecting the optimal power allocation ratio k, the system can much reduce the outage probability compared with the case of the equal power allocation when the relay is allocated near to the destination, while they achieve almost the same outage when relay is near to the source.

2.1.4.3 Optimal Power Allocation: Outage Probability Requirement Fixed

In this sub-section, we investigate how much total transmit power can be saved through optimal power allocation, given a fixed outage probability requirement. The problem can be formulated as

$$\begin{aligned} \underset{k,E_{\mathrm{T}}}{\text{minimize}} \quad & E_{\mathrm{T}} \\ \text{subject to} \quad & P_{out}(k,E_{\mathrm{T}}) - T_{out} \leq 0 \\ & k-1<0 \\ & -k<0 \\ & -E_{\mathrm{T}}<0, \end{aligned} \tag{2.20}$$

where T_{out} is required outage probability. The convexity of (2.20) is proven in sub-section 2.1.4.1.

Tables 2.2 and 2.3 show the required total transmit power with equal and optimal power allocations for outage requirements, where d_r is 0.6 and 0.7, respectively. The outage probability requirements are set as $P_{out} =$

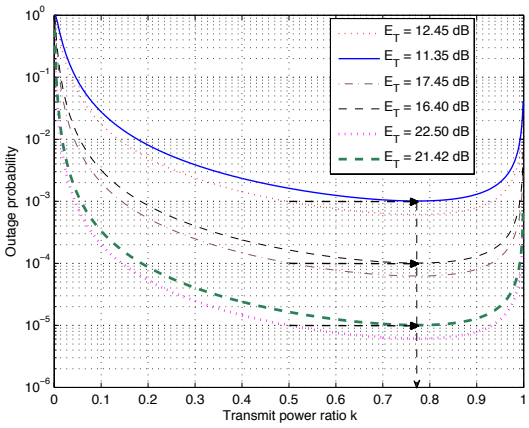

Figure 2.6: Theoretical outage probabilities versus the optimal power ratio k with different total transmit powers, d_r = 0.6.

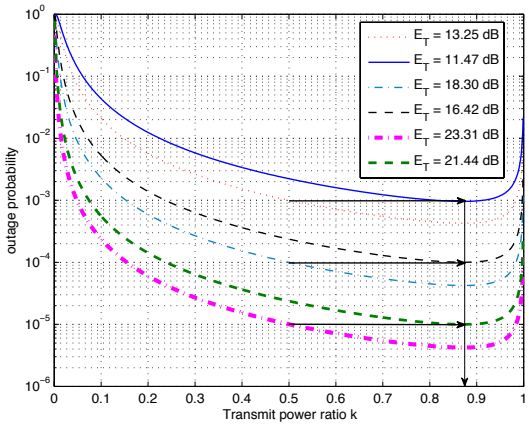

Figure 2.7: Theoretical outage probabilities versus the optimal power ratio k with different total transmit powers, d_r = 0.7.

$10^{-5}, 10^{-4}, 10^{-3}$, respectively. It is clearly seen that by selecting the optimal k values, roughly 1$\sim$2 dB gain can be achieved by optimal power allocation compared with that with equal power allocation. It is also found that, given the relay location, the transmit power gains with the optimal power allocation over the equal power allocation are almost the same, regardless of the outage requirements. As shown in Fig. 2.6 and Fig. 2.7, the optimal k values corresponding to outage requirements are exactly consistent to the the data obtained as the solution to the optimization problem.

2.1.5 Impact of LOS component on optimal power allocation

In this sub-section, we focus on the impact of the LOS components on the outage probability of the LosFoR system defined in Fig. 2.1. The S-D link is assumed to suffer from block Rayleigh fading while the R-D and S-R links from block Rician fading. The pdf of the instantaneous SNR γ_i $(i = 2,3)$ following Rician distribution is given by

$$p^{Rici}(\gamma_i) = \left(\frac{(1+K_i)\,e^{-K_i}}{\Gamma_i}\right) \exp\left(-\frac{(1+K_i)\gamma_i}{\Gamma_i}\right) I_0\left(2\sqrt{\frac{K_i\,(1+K_i)\,\gamma_i}{\Gamma_i}}\right), \tag{2.21}$$

where $\Gamma_i (i = 2,3)$ represent received average SNRs of the R-D and S-R channels, respectively. $I_0(\cdot)$ is the zero-th order modified Bessel function of the first kind, and K_i denotes the ratio of the LOS component power-to-non-LOS components average power for the corresponding links. K_i represents the severity of fading. With $K_i = \infty$, the

Table 2.2: Optimal power ratio k with fixed P_{out} (d_r=0.6)

required P_{out}	required E_{T} (equal power)	required E_{T} (optimal power)	Gain
0.001	12.45 dB	11.35 dB (k=0.774)	1.1 dB
0.0001	17.45 dB	16.40 dB (k=0.774)	1.05 dB
0.00001	20.50 dB	21.42 dB (k=0.774)	1.08 dB

Table 2.3: Optimal power ratio k with fixed P_{out} (d_r=0.7)

required P_{out}	required E_{T} (equal power)	required E_{T} (optimal power)	Gain
0.001	13.25 dB	11.47 dB (k=0.871)	1.88 dB
0.0001	18.30 dB	16.42 dB (k=0.872)	1.88 dB
0.00001	23.31 dB	21.44 dB (k=0.872)	1.87 dB

channel is equivalent to a static additive white Gaussian noise (AWGN) channel, and with $K_i = 0$ the channel reduces to Rayleigh fading channel.

Based on the same definition of outage probability in previous section, the outage probabilities of the LosFoR system with the fading variation of the S-R and R-D links following the Rician distribution can then be expressed

$$\begin{aligned} P_1^{Rici} &= \int_{\gamma_1=0}^{1}\int_{\gamma_2=0}^{2^{1-\log_2(1+\gamma_1)}-1}\int_{\gamma_3=1}^{\infty} p(\gamma_1)p^{Rici}(\gamma_2)p^{Rici}(\gamma_3)d\gamma_1 d\gamma_2 d\gamma_3 \\ &= Q_1\left(\sqrt{2K_3},\sqrt{\frac{2(1+K_3)}{\Gamma_3}}\right)\int_1^{\gamma_1=0}\frac{1}{\Gamma_1}\exp\left(-\frac{\gamma_1}{\Gamma_1}\right)\cdot\left[1-Q_1\left(\sqrt{2K_2},\sqrt{2(1+K_2)\frac{2^{1-\log_2(1+\gamma_1)}-1}{\Gamma_2}}\right)\right]d\gamma_1, \end{aligned} \tag{2.22}$$

$$\begin{aligned} P_2^{Rici} &= \int_{\gamma_1=0}^{2^{H(pe)}-1}\int_{\gamma_2=0}^{\infty}\int_{\gamma_3=0}^{1} p(\gamma_1)p^{Rici}(\gamma_2)p^{Rici}(\gamma_3)d\gamma_1 d\gamma_2 d\gamma_3 \\ &= \int_{\gamma_3=0}^{1}\exp\left(-\frac{(1+K_3)\gamma_3}{\Gamma_3}\right)\left(\frac{(1+K_3)e^{-K_3}}{\Gamma_3}\right)I_0\left(2\sqrt{\frac{K_3(1+K_3)\gamma_3}{\Gamma_3}}\right)\cdot\left[1-\exp\left(-\frac{2^{1-\log_2(1+\gamma_3)}-1}{\Gamma_1}\right)\right]d\gamma_3, \end{aligned} \tag{2.23}$$

$$\begin{aligned} P_3^{Rici} &= \int_{\gamma_1=2^{H(pe)}-1}^{1}\int_{\gamma_2=0}^{2^{1+H(pe)-\log_2(1+\gamma_1)}-1}\int_{\gamma_3=0}^{1} p(\gamma_1)p^{Rici}(\gamma_2)p^{Rici}(\gamma_3)d\gamma_1 d\gamma_2 d\gamma_3, \\ &= \frac{1}{\Gamma_1}\int_{\gamma_1=2^{1-\log_2(1+\gamma_3)-1}}^{1}\int_{\gamma_3=0}^{1}\exp\left(-\frac{\gamma_1}{\Gamma_1}\right)\exp\left(-\frac{(1+K_3)\gamma_3}{\Gamma_3}\right)\left(\frac{(1+K_3)e^{-K_3}}{\Gamma_3}\right)I_0\left(2\sqrt{\frac{K_3(1+K_3)\gamma_3}{\Gamma_3}}\right) \\ &\quad\cdot\left[1-Q_1\left(\sqrt{2K_2},\sqrt{2(1+K_2)\frac{2^{2-\log_2(1+\gamma_3)-\log_2(1+\gamma_1)}-1}{\Gamma_2}}\right)\right]d\gamma_1 d\gamma_3, \end{aligned} \tag{2.24}$$

where $Q_1(\cdot,\cdot)$ is the Marcum Q-Function.

We follow the same strategy as in previous section, where all links are assumed Rayleigh fading channels, to minimize the outage probability. The total transmit power E_T is fixed and the noise variance ${\sigma_n}^2$ of each channel

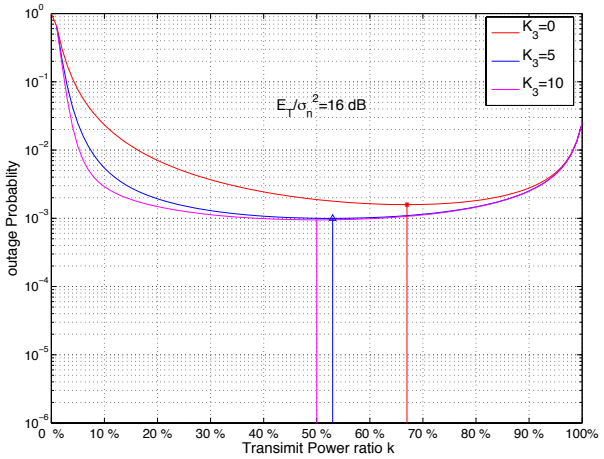

Figure 2.8: Theoretical outage probabilities versus the optimal power ratio k with different Rician factor K_3 in S-R channel.

is normalized to unity. The transmit power, which is equivalent to their corresponding average SNR, allocated to S and R are denoted as kE_T and $(1-k)E_T$, respectively, where k ($0 < k < 1$) is power allocation ratio.

Since the presence of Marcum Q-Function and zero-th order modified Bessel function in outage expressions, derivation of the explicit closed-form expression of (2.22), (2.23) and (2.24) may be excessively complex. The recursive adaptive Simpson quadrature algorithm [GG00] can be used to numerically calculate the integrals of P_1^{Rici}, P_2^{Rici} and P_3^{Rici}.

Fig. 2.8 illustrates the outage probability curves with different Rician factor K_3 values for S-R channel while Rician factor K_2 for R-D equals to zero, and $E_T/{\sigma_n}^2 = 16$ dB. The x-axis represents the ratio k of transmit power allocated to S. The 100% point indicates that transmit power is totally allocated to S, and 50% point represents the transmit power is allocated to both sources equally. It is found from Figure 2.8 that the optimal power ratio k that achieves the minimum outage probability decreases as the value of K_3 increases. This is reasonable because when the fading variation of S-R channel reduce, we should allocate more power to the R which decodes $\mathbf{b}_2$ with higher successful ratio.

Figure 2.9 shows the power allocation ratio k versus the outage probability with the Rician factor K_2 values for R-D channel as a parameter for $E_T/{\sigma_n}^2 = 16$ dB, while Rician factor $K_3 = 0$. It should be noted that the optimal k value, that achieves the smallest outage probability is increased as the K_2 value is increased. This indicates that the larger the ratio of LOS component in R-D channel, the less the outage probability. However, more transmit power needs to be allocated to S even though R-D channel is under milder fading condition. This is because the deep fading in S-R channel ($K_3 = 0$) results in high decoding error in R. $\mathbf{b}_2$ is transmitted successfully over R-D having strong LOS component even though $\mathbf{b}_2 \neq \mathbf{b}_1$. This indicates that allocating more power to R cannot help to improve the outage performance. On the contrary, it is more effective to allocate more power to S than to R in such scenario.

Figure 2.10 shows the impact of the Rician factor K_2 and K_3 on the outage probability simultaneously. It is found that by increasing the values of K_2 and K_3 simultaneously, significant outage gain can be achieved. Similarly to the case when only K_3 becomes larger, optimal power ratio k that achieves the minimum outage probability becomes small as the value of K_2 and K_3 become larger simultaneously. This is because the decrease of fading variation in S-R improve the decoding success ratio at R. Furthermore, $\mathbf{b}_2$ benefit from the increase of LOS power ratio in R-D channel. Therefore the lowest outage probability can be achieved when the contribution of the S-R and R-D channels are balanced.

2.1.6 Summary

This section has investigated the optimal power allocation for a LosFoR system based on outage probability analysis. In the proposed system model, besides the S-D and R-D channels, the S-R channel is also assumed to suffer

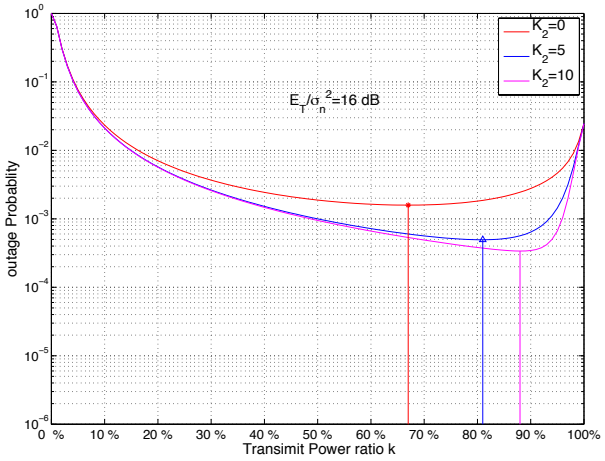

Figure 2.9: Theoretical outage probabilities versus the optimal power ratio k with different Rician factor K_2 in R-D channel.

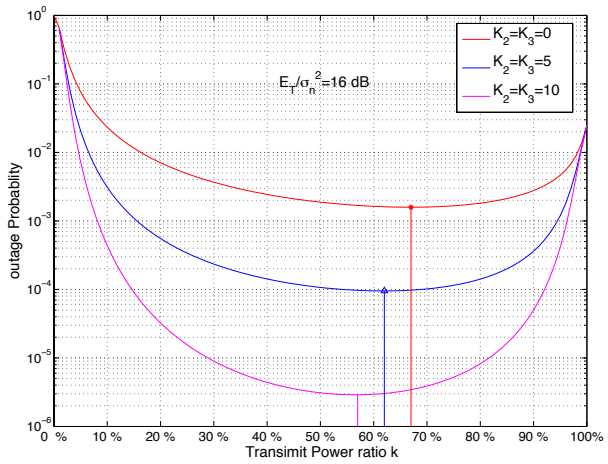

Figure 2.10: Theoretical outage probabilities versus the optimal power ratio k with different Rician factor $K_3(=K_2)$ in S-R and R-D channel.

from block Rayleigh fading and is modelled by the rate distortion function in lossy scenario. An approximated closed-form expression of outage probability for the LosFoR system has been derived, where the geometrical gain is taken into account. As shown in the results, the proposed approximation can ensure sufficient accuracy of the outage probability calculation. Based on the expression, the optimal power allocation scheme has been formulated as a convex problem for minimizing the outage probability while keeping the total transmit power constant, and for minimizing the transmit power while keeping the outage probability fixed. Compared with equal power allocation, by adjusting the power allocated to S and R, lower outage probability can be achieved. Moreover, it has been shown that when R is near to D, the proposed optimization scheme can achieve much lower outage probability than that with the equal power allocation. This section also has investigated the impact of the LOS component on optimal power allocation for the LosFoR system.

2.2 Relay-Oriented Source Power Allocation for MIMO Selective-DF Relaying System

2.2.1 Motivation and Objective

In this section, we exploit a relay-oriented source power allocation algorithm for MIMO selective-DF (S-DF) relaying network in order to enhance the system spectrum efficiency. Consider a two-hop MIMO relaying network, where the system consists of a multi-antenna based source node, a multi-antenna based relay node, and K single-antenna based destination nodes. Without the global channel state information (CSI) to be assumed at each node, joint power allocation and beamforming design in order to maximize the system performance seems extremely difficult. In this case, the conventional MIMO S-DF relaying strategy normally allows the source node optimize its precoding matrix based on its direct channel links to its served destination nodes. Meanwhile, if the SNR or the signal-to-interference-plus-noise ratio (SINR) of certain received data streams at relay node can pass the predetermined threshold, the relay node will forward the data streams to the destination nodes in order to help the source node improve the system performances [LTW04; NBK04; BK13]. However, such strategy may loss the system optimality if the source node has the location and power budget information of the relay node.

Motivated by the above discussion, with only the local CSI to be assumed at each node, a relay-oriented source power allocation algorithm is proposed in order to improve the system performance. In detail, instead of optimizing the transmission power to increase the performance between its direct links to the destination nodes, the source node firstly allocates its transmission power aiming to allow as much as the data streams' SNR/SINR at the relay node pass the predetermined threshold. Then, if there is still some power left, the source node will allocate the residual power for its direct links to the destination nodes in order to further increase the system performance. Subsequently, the relay node will formulate the precoding matrix for its selected data streams and forward the messages to the corresponding destination nodes. Simulation results show that the proposed power allocation algorithm can exhibit better sum-rate and bit error rate performances by comparing with the conventional MIMO S-DF relaying scheme, especially when the relay node is placed in the middle of source node and the destination nodes.

2.2.2 System Model

An example of a two-hop MIMO S-DF relaying network is given by Fig.2.11. As shown in Fig. 2.11, the source

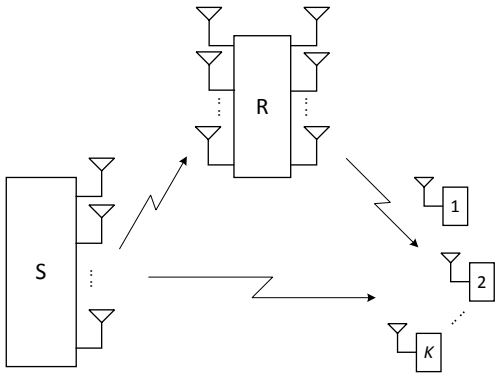

Figure 2.11: System model of MIMO S-DF relaying network.

node (S) deployed with M_b transmit antennas serves K single-antenna based destination nodes ($\mathrm{D}_i, i = 1,\ldots,K$) with the help of M_r antennas based relay node (R). The relay node is placed in a position between the source node and the destination nodes, and its operation is performed in a half duplex mode, where the entire communication process can be divided into two phases. In the first phase, the source node broadcasts multiple data streams to the K destination nodes and the relay node; In the second phase, the relay node decodes certain received signal and forwards the re-encoded symbols to the corresponding destination nodes. Here, the threshold based S-DF strategy is implemented at the relay node, and both phases span the same time duration.

Consider that the system works in narrowband. Each the node can only obtain the CSI regarding to its own links

(i.e., the local CSI), where the CSI is obtained through either the channel reciprocity for the TDD mode or the limited feedback for the FDD mode. Denote that $\mathbf{W}$ with the size of $M_b \times K$ $(M_b \geq K)$ is the precoding matrix at the source node. In the first phase, the discrete-time equivalent form of received signal at the k^{th} destination node can be expressed as

$$y_{k,b} = \mathbf{h}_{k,b}^T \mathbf{W} \mathbf{s}_b + v_1, \tag{2.25}$$

where $\mathbf{s}_b \in \mathbb{R}^{K\times 1}$ is the vector of transmitted data streams subject to the transmission power constraint P_b, i.e., $E\{\|\mathbf{s}_b\|^2\} \triangleq \sum_{k=1}^{K} \sigma_{k,b}^2 \leq P_b$, here, $\sigma_{k,b}^2$ is the transmission power allocated to the k^{th} data stream at the source node; $\mathbf{h}_{k,b} \in \mathbb{C}^{M_b\times 1}$ is the channel vector from the source node to the k^{th} destination node; v_1 is the independent and identically distributed (i.i.d.) AWGN with zero mean and variance σ_0^2. Meanwhile, the discrete-time equivalent form of received signal after the decoding process at the relay node can be expressed as

$$\begin{aligned} \widetilde{\mathbf{y}}_{rb} &= \mathbf{U}^H \mathbf{y}_{rb} \\ &= \mathbf{U}^H \mathbf{H}_{rb} \mathbf{W} \mathbf{s}_b + \mathbf{U}^H \mathbf{v}_r, \end{aligned} \tag{2.26}$$

where $\mathbf{H}_{rb} \in \mathbb{C}^{M_r\times M_b}$ is the channel matrix from the source node to the relay node; $\mathbf{U}$ with the size of $M_r \times K$ $(M_r \geq K)$ is the decoding matrix at the relay node; $\mathbf{v}_r$ is the i.i.d. AWGN vector with zero mean and covariance matrix $\sigma_0^2\mathbf{I}$.

Denote that $\mathbf{T}$ with the size of $M_r \times K$ $(M_r \geq K)$ is the precoding matrix at the relay node. Hence, in the second phase, the discrete-time equivalent form of received signal at the k^{th} destination node then can be expressed as

$$y_{k,r} = \mathbf{h}_{k,r}^T \mathbf{T} \mathbf{s}_r + v_2, \tag{2.27}$$

where $\mathbf{s}_r \in \mathbb{R}^{K\times 1}$ is the vector of transmitted data streams subject to the transmission power constraint P_r, i.e., $E\{\|\mathbf{s}_r\|^2\} = \sum_{l=1}^{K} \sigma_{k,r}^2 \leq P_r$, here, $\sigma_{k,r}^2$ is the transmit power allocated to the k^{th} data stream at the relay node; $\mathbf{h}_{k,r} \in \mathbb{C}^{M_r\times 1}$ is the channel vector from the relay node to the k^{th} destination node; v_2 is the i.i.d. AWGN with zero mean and variance σ_0^2. It is worthwhile to note that, following the S-DF strategy, the transmit power of unselected data streams at the relay node need to be set up to zeros, and the corresponding destination node in the second phase needs to stop receiving signals.

2.2.3 Precoding/Decoding Matrices Design and Problem Formulation

The precoding and decoding matrices as mentioned above are used to mitigate the multiuser/inter-stream interference and achieve the system sum-rate performance. Such matrices can be designed based on the dirty paper coding [Cos83] and/or maximum-likelihood principle [Ver98] at the cost of exponentially complexity, which is not efficient for the hardware implementation [ZMG+09]. In order to reduce the precoding and decoding complexity, the linear based precoding and decoding design are favoured, e.g., zero-forcing (ZF). In this section, we are mainly focusing on ZF based precoding and decoding matrices design for the multiuser/inter-stream interference mitigation.

Start from the precoding matrix $\mathbf{W}$ formulation at the source node. Our aim is to use it to completely eliminate the multiuser interference among all K destination nodes in the first phase. With the channel information $\mathbf{h}_{k,b}, \forall k$, at the source node, such precoding matrix can be formulated as

$$\mathbf{W} = \underbrace{\mathbf{H}_b^H \left(\mathbf{H}_b \mathbf{H}_b^H\right)^{-1}}_{\triangleq \widetilde{\mathbf{W}}} \boldsymbol{\beta}, \tag{2.28}$$

where $\mathbf{H}_b \triangleq \left[\mathbf{h}_{1,b}^T; \ldots; \mathbf{h}_{K,b}^T\right]$ is the channel matrix from the source node to all K destination nodes; $\boldsymbol{\beta} = \text{diag}\{\beta_1, \ldots, \beta_K\}$ is a diagonal matrix for achieving the power constraint on the precoding matrix $\mathbf{W}$, here, we have

$$\beta_k = \sqrt{\frac{1}{\text{trace}\left(\widetilde{\mathbf{w}}_k \widetilde{\mathbf{w}}_k^H\right)}}, \; k = 1, \ldots, K, \tag{2.29}$$

where $\widetilde{\mathbf{w}}_k$ is the k^{th} column of $\widetilde{\mathbf{W}}$.

According to (2.26), the received signal at the relay node needs to go though the decoding matrix $\mathbf{U}$ to eliminate the inter-stream interference at the relay node. Denote that $\mathbf{A} \triangleq \mathbf{H}_{rb}\mathbf{W}$, hence, the decoding matrix $\mathbf{U}$ can be formulated as

$$\mathbf{U} = \mathbf{A}\left(\mathbf{A}^H\mathbf{A}\right)^{-1}. \tag{2.30}$$

Then, according to the S-DF strategy, the SNR of the k^{th} received data stream after the decoding process at the relay node can be expressed as

$$\text{SNR}_k = \frac{\sigma_{k,b}^2}{\sigma_0^2 \left\|\mathbf{u}_k\right\|^2}, \tag{2.31}$$

where $\mathbf{u}_k$ is the k^{th} column of the decoding matrix $\mathbf{U}$ at the relay node. By setting up the pre-determined threshold, we aim at comparing each data stream's SNR (i.e., see (2.31)) with the pre-determined threshold, and only the data streams whose SNRs can pass the pre-determined threshold will be re-encoded and forwarded to the corresponding destination nodes. Here, the precoding matrix $\mathbf{T}$ at the relay node can be formulated by following the way in (2.31) and (2.32), and as we mentioned, the transmit power of all the unselected data streams in this case will be set up to zero.

Following the above described precoding/decoding matrices design, all the multiuser/inter-stream interference can be completely removed. Then, the efficient power allocation algorithm needs to be designed to guarantee the system performance. In other words, the main objective of the work is to

$$\begin{array}{ll} \underset{\sigma_{k,b}^2,\sigma_{k,r}^2}{\text{maximize}} & \frac{1}{2}\sum_{k=1}^{K}\log\left(1+\frac{\sigma_{k,b}^2|\mathbf{h}_{k,b}^T\mathbf{w}_k|^2+\sigma_{k,r}^2|\mathbf{h}_{k,r}^T\mathbf{t}_k|^2}{\sigma_0^2}\right) \\ \text{subject to} & \sum_{k=1}^{K}\sigma_{k,b}^2 \le P_b,\ \sum_{k=1}^{K}\sigma_{k,r}^2 \le P_r, \end{array} \tag{2.32}$$

where $\mathbf{w}_k$ and $\mathbf{t}_k$ with unit norm are the k^{th} column of $\mathbf{W}$ and $\mathbf{T}$, respectively.

2.2.4 The Proposed Relay-Oriented Source Power Allocation Algorithm

Assume that each node can only has the CSI related to its own links. In this case, the conventional MIMO S-DF relaying strategy allows the source node optimizing its transmission power based on the direct channel links between itself and its served destination nodes. Here, the relay node might help if its received signal strength from the source node can pass the pre-determined threshold, where the decoding errors can be controlled. In general, such strategy may lose the system optimality if the source node has the location information about the relay node. For example, if the relay node is in the middle of the source node and the destination nodes, why not allocate the source's transmission power to let more data streams' SNRs at the relay node pass the pre-determined threshold, which allow the relay node to provide its maximum help.

Motivated by this, the proposed relay-oriented source power allocation strategy is to maximize the number of data streams whose SNRs at the relay node can pass the pre-determined threshold, and utilize the residual power for the source's direct link optimization. In detail, start from sorting the inverse of the noise power of all the data streams received at the relay node after the decoding process. Without loss of generality, we give an example assuming that

$$\frac{1}{\sigma_0^2\left\|\mathbf{u}_1\right\|^2} \ge \cdots \ge \frac{1}{\sigma_0^2\left\|\mathbf{u}_K\right\|^2}. \tag{2.33}$$

As we know, each node can only have its related channel knowledge. Hence, after the sorting process, the source node can allocate its transmission power P_b starting from the data stream, which has the largest value of the inverse of the noise power (i.e., the 1st term in (2.33)). Assume that SNRT is the pre-determined threshold that is used to select the data stream(s) at the relay node. Hence, we suppose to allocate the transmission power to the 1st data stream in order to satisfy

$$\frac{\widetilde{\sigma}_{1,b}^2}{\sigma_0^2\left\|\mathbf{u}_1\right\|^2} = \text{SNRT}, \tag{2.34}$$

where $\widetilde{\sigma}_{1,b}^2$ denotes the transmission power allocated to the 1st data stream in order to pass SNRT at the relay node. In this case, if $\widetilde{\sigma}_{1,b}^2 < P_b$, the residual power $(P_b - \widetilde{\sigma}_{1,b}^2)$ will be used to allocate to the next data stream which has the second largest value of the inverse of the noise power in (2.33); If $\widetilde{\sigma}_{1,b}^2 > P_b$, which means that P_b cannot let

even one data stream pass SNRT, thus the system will not let the relay help. To sum up, there are some cases could happen after the relay-oriented source power allocation process:

Case 1: There are some/all data streams' SNRs at the relay node passing SNRT, but all the transmission power at the source node has been used;

Case 2: There are some/all data streams' SNRs at the relay node passing SNRT, and there is still some residual power left;

Case 3: There is no data stream's SNR at the relay node passing SNRT.

For *Case 1*, all the transmission power has been used to let some/all data streams' SNRs at the relay node passing SNRT, and there is no additional power left to be allocated to further enhance the channel links between the source node and the destination nodes. For *Case 3*, the relay node cannot help, hence, the conventional water-filling power allocation algorithm (e.g., see [Gol05]) for the channel links between the source node and all the destination nodes can be implemented in order to maximize the system performance.

For *Case 2*, in one scenario, the SNRs of some data streams at the relay node can pass SNRT, but the residual power cannot let an additional data stream's SNR pass SNRT; in the other scenario, the SNRs of all the data streams at the relay node can pass SNRT, and there is still some residual power left. For both scenarios, the residual power can be used to further enhance the performance of the channel links between the source node and its served destination nodes. Specifically, assume that there are L ($\leq K$) number of the data streams' SNRs at the relay node that can pass SNRT, and following the assumption in (2.33), the residual power can be formulated by

$$\begin{aligned} P_{\text{res},b} &= P_b - \sum_{l=1}^{L} \widetilde{\sigma}_{l,b}^2 \\ &= P_b - \sum_{l=1}^{L} \sigma_0^2 \left\|\mathbf{u}_l\right\|^2 \cdot \text{SNRT}, \end{aligned} \tag{2.35}$$

where $P_{\text{res},b}$ can be used to further enhance the performance of the channel links between the source node and the destination nodes. In detail, after the source node allocating $\sum_{l=1}^{L} \widetilde{\sigma}_{l,b}^2$ transmission power to let L data streams' SNRs pass SNRT, the corresponding allocated power for the data streams will be fixed, and accompanied with the $(K-L)$ data streams which have not been allocated by any power, we will use the residual power $P_{\text{res},b}$ to

$$\begin{array}{ll} \underset{\varepsilon_l}{\text{maximize}} & \sum_{l=1}^{L} \log\left(1+\frac{\varepsilon_l|\mathbf{h}_l^T\mathbf{w}_l|^2+\widetilde{\sigma}_{l,b}^2|\mathbf{h}_l^T\mathbf{w}_l|^2}{\sigma_0^2}\right) + \sum_{l=L+1}^{K} \log\left(1+\frac{\varepsilon_l|\mathbf{h}_l^T\mathbf{w}_l|^2}{\sigma_0^2}\right) \\ \text{subject to} & \sum_{l=1}^{K} \varepsilon_l = P_{\text{res},b}, \end{array} \tag{2.36}$$

where ε_l is the additional power spend on the l^{th} data stream, and the total power spend on the l^{th} data stream at the source node is $\sigma_{l,b}^2 = \widetilde{\sigma}_{l,b}^2 + \varepsilon_l$ for $l \in \{1,\ldots,L\}$ or $\sigma_{l,b}^2 = \varepsilon_l$ for $l \in \{(L+1),\ldots,K\}$. Here, the problem (2.36) can be solved based on the Lagrangian duality theory in [BV04; Gol05].

To sum up, the proposed relay-oriented source power allocation algorithm can be described as:

Relay-Oriented Source Power Allocation Algorithm

I. Sort $1/(\sigma_0^2 \|\mathbf{u}_k\|^2), \forall k$, in a descent order, and set $i = 1$;
II. **If** $\widetilde{\sigma}_{i,b}^2 > P_b$, *Case 3* happens, the water-filling power allocation algorithm in [Gol05] is implemented for the channel links between the source node and the destination nodes, **return**;
III. **If** $\widetilde{\sigma}_{i,b}^2 = P_b$, *Case 1* happens, **return**;
VI. **If** $\widetilde{\sigma}_{i,b}^2 < P_b$, $\widetilde{\sigma}_{i,b}^2 = \sigma_0^2 \|\mathbf{u}_i\|^2 \cdot \text{SNRT}$;
V. **While** $i \leq K$:
1. Increasing i by 1;
2. **If** $\widetilde{\sigma}_{i,b}^2 > P_b - \sum_{l=1}^{i-1} \widetilde{\sigma}_{l,b}^2$, *Case 2* happens, let $P_{\text{res},b} = P_b - \sum_{l=1}^{i-1} \widetilde{\sigma}_{l,b}^2$, solve (2.36), **break**;
3. **If** $\widetilde{\sigma}_{i,b}^2 = P_b - \sum_{l=1}^{i-1} \widetilde{\sigma}_{l,b}^2$, *Case 1* happens, **break**;
4. **If** $\widetilde{\sigma}_{i,b}^2 < P_b - \sum_{l=1}^{i-1} \widetilde{\sigma}_{l,b}^2$, $\widetilde{\sigma}_{i,b}^2 = \sigma_0^2 \|\mathbf{u}_i\|^2 \cdot \text{SNRT}$, **goto** Step V-1;
End While

The worst-case computational complexity of proposed power allocation algorithm can be analyzed as: For Step I, the sorting process takes $\mathcal{O}\{K^2\}$ complexity, where K is the total number of the data streams; For Step II, if the condition is satisfied, the conventional water-filling algorithm is implemented, and the algorithm takes $\mathcal{O}\{K^3\}$ complexity as shown in [Gol05]; For Step V-2, solving (2.36) also takes $\mathcal{O}\{K^3\}$ complexity; Apart from these, all the rest steps are just some linear additions and scalar multiplications, where their complexity are less than $\mathcal{O}\{K^3\}$. Hence, the computational complexity of the proposed algorithm is $\mathcal{O}\{K^3\}$, which is the cubic complexity.

2.2.5 Simulation Results

Computer simulations were used to evaluate the proposed relay-oriented source power allocation algorithm in terms of sum-rate and bit error rate. All the channels were generated as independent Rayleigh fading, which remained static over the transmission of each block. Assumed that the source node was equipped with $M_b = 4$ transmit antennas serving $K = 4$ destination nodes with the help of $M_r = 4$ antenna based relay node. The SNR was defined as the transmission power normalized by noise power ratio, where both the source node and the relay node have the same power constraint (i.e., $P_b = P_r$). There were two baselines for comparison: For the first one (Baseline I), the source node optimized its transmission power for the direct link to its served destination nodes, and the relay node would help if its received data streams' SNRs can pass the pre-determined threshold (i.e., SNRT=1 dB); For the second one (Baseline II), equal power allocation was implemented to all activated data streams at both source and relay nodes.

Given the distance between the source node and the destination nodes, e.g., $d_{\text{sd}}^{(k)} = d, \forall k$, the sum-rate performances of different schemes are presented based on two relay locations. For *Location A*, the distance between the source node and the relay node (e.g. d_{sr}), and the distance between the relay node and the destination nodes (e.g., $d_{\text{rd}}^{(k)}, \forall k$) are the same as d, where $d_{\text{sr}} = d_{\text{rd}}^{(k)} = d, \forall k$; For *Location B*, the relay node is placed in the middle of the source node and the destination nodes, where $d_{\text{sr}} = d_{\text{rd}}^{(k)} = d/2, \forall k$. Following the work in [YG11], the SNRs of the three types of channels, e.g., SNR_{sd}, SNR_{sr} and $\text{SNR}_{\text{rd}}^{(k)}, \forall k$, for the two relay locations can be approximated by: (A) $\text{SNR}_{\text{sr}} = \text{SNR}_{\text{rd}}^{(k)} = \text{SNR}_{\text{sd}}, \forall k$; (B) $\text{SNR}_{\text{sr}} = \text{SNR}_{\text{rd}}^{(k)} = \text{SNR}_{\text{sd}} + 10.6 \text{ dB}, \forall k$.

Fig. 2.12 shows the sum-rate performances of different schemes with the two relay locations. As shown in the figure, for *Location A*, the sum-rate performance of proposed algorithm is near the same as the one of Baseline I when the SNR_{sd} values are low. This is because, in this case, few data streams' SNRs at the relay node can pass SNRT, and all the transmission power at the source will be allocated to the channel links between the source node and the destination nodes. In contrast, at high SNR_{sd} range, the proposed algorithm for *Location A* outperforms Baseline I & II, and, as expected, the performances of Baseline I & II are converged to each other; For *Location B*, the proposed algorithm outperforms both baselines around 2 bit/s/Hz throughout the whole given SNR_{sd} range. The reason is because that, in this case, the SNRs of many data streams at the relay node can pass SNRT, where the proposed algorithm is able to be implemented to let the relay node provide the maximum help.

Fig. 2.13 shows the bit-error-rate performances of different schemes with the two relay locations. Referring

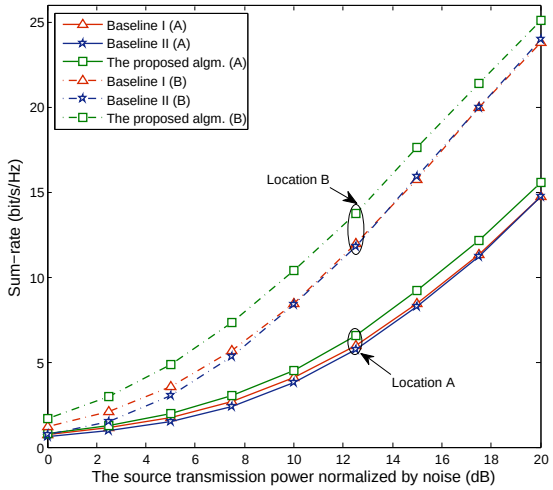

Figure 2.12: Sum-rate vs. the source's transmission power normalized by noise. Comparing the different schemes for two relay locations.

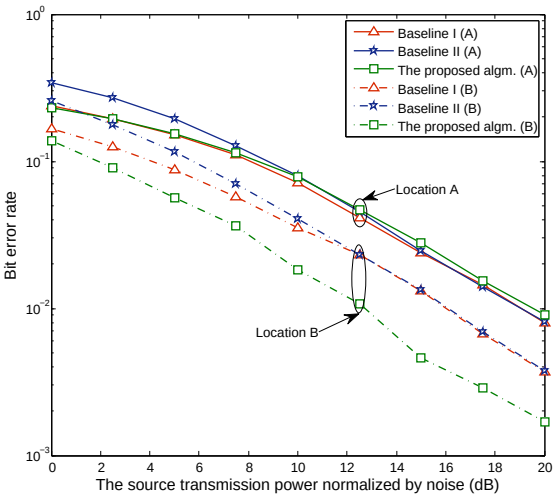

Figure 2.13: Bit-error-rate vs. the source's transmission power normalized by noise. Comparing the different schemes for two relay locations.

to D2.1.1, here, we also include turbo-like channel coding and quadrature phase-shift keying modulation in the system. Specifically, the $1/2$ rate serial concatenated convolutional code is implemented at the source node, where the first encoder is the non-recursive non-systematic convolutional code with a generator polynomial $G = ([3,2])_8$, after the random interleaver with the length of 1000, the second encoder is the doped-accumulator with a doping rate $P_s = 1$. At the relay node, after passing $\mathbf{U}$, the selected data streams are firstly decoded according to single iteration based turbo decoders with Bahl-Cocke-Jelinek-Raviv (BCJR) algorithm [BCJ+74], and then the same encoders as used at the source node are implemented to re-encode and forward the selected data streams to the users. Each destination node, after the soft demodulation, linearly combines the received bits' log likelihood ratios from the source node and the relay node, and then decodes the data streams according to up to 50 iteration based turbo decoders with BCJR algorithm.

As shown in Fig 2.13, for *Location A*, similar as the sum-rate performance, the proposed algorithm has the same bit error rate performance as Baseline I when $\mathrm{SNR}_{\mathrm{sd}}$ is low. However, when $\mathrm{SNR}_{\mathrm{sd}}$ is high, the bit error rate performance of the proposed algorithm is a bit worse than Baseline I & II. This is because that, in order to simplify the decoding process, only one iteration is implemented for turbo decoding at the relay node. In this case, even the proposed algorithm tries to allow more data streams to pass the pre-determined threshold SNRT, there still exist certain amount of decoding errors and will be forwarded to the destination nodes. Such kind of error propagation can hardly happen when the relay node is placed in *Location B*. That is why the proposed algorithm in *Location B*,

as expected, has much better bit-error-rate performance by comparing with the two baselines throughout the whole given SNR_{sd} range.

2.2.6 Summary

In this section, a relay-oriented source power allocation algorithm for MIMO S-DF relaying has been developed to maximize the system performance under the total power constraints. The proposed algorithm featured the cubic computational complexity. Simulation results have shown that, without the global channel knowledge at the source node, the proposed algorithm outperforms the conventional MIMO S-DF relaying schemes in terms of sum-rate and bit-error-rate, especially when the relay node is placed in the middle of the source node and the destination nodes.

3. Power Allocation for Chief Executive Officer (CEO) Problem

3.1 Outage Based Power Allocation for CEO Problem

In this section, we minimize the outage probability for TS2 also referred to as CEO problem [BZH96]. It is shown that the outage probability can be approximated as a convex function and thus, convex optimization can be applied to find the optimal solution.

3.1.1 System Model

Fig. 3.1 represents the system model, where an i.i.d. binary Bernoulli information sequence $\mathbf{b}_0$ is originated by the source (S) with $\Pr[\mathbf{b}_0 = 0] = \Pr[\mathbf{b}_0 = 1] = 0.5$. The information sequence is corrupted by independent binary Bernoulli distributed errors $\mathbf{e}_i$ via BSCs. The information sequence $\mathbf{b}_i = \mathbf{b}_0 \oplus \mathbf{e}_i$, $i \in \{1,2,3\}$ is observed by relay (R) i and can be associated with the bit flipping probability $p_i = \Pr[\mathbf{e}_i = 1]$ and $p_i \in (0, 0.5)$. "$\oplus$" denotes the binary exclusive OR operation. The correlated information sequences $\mathbf{b}_i, \forall i$ are transmitted via Rayleigh fading channels to the destination (D). The PDF of the Rayleigh fading channel is given by

$$p(\gamma_i) = \frac{1}{\Gamma_i} \exp(-\frac{\gamma_i}{\Gamma_i}), \forall i, \tag{3.1}$$

with instantaneous SNR γ_i and average SNR

$$\Gamma_i = \frac{E_\mathrm{i}}{N_0} \cdot d_i^{-\eta}, \tag{3.2}$$

where E_i is the transmit power of relay i, N_0 is the variance of AWGN, d_i the distance between relay i and destination and η the path loss exponent. Best performed recovery of $\hat{\mathbf{b}}_0$ at the destination can by achieved if all information sequences $\hat{\mathbf{b}}_1$, $\hat{\mathbf{b}}_2$ and $\hat{\mathbf{b}}_3$ are recovered error free [WMF15].

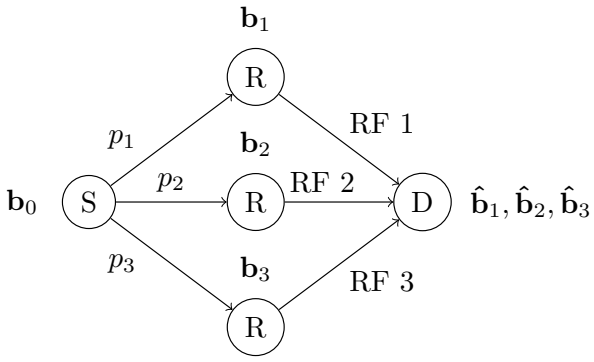

Figure 3.1: System model for CEO Problem.

If at least one relay information sequence cannot be recovered error-free, the information recovery of the source is considered to be unsuccessful, also referred to as outage. In chapter "Slepian-Wolf Admissible Rate Region Based Outage Probability Derivation for CEO Problem" of deliverable D1.2.1, the outage probability for high-SNR of the system model is derived and can be approximated as

$$P_{out} \approx \frac{C_1 - 1}{\Gamma_1} + \frac{C_2 - 1}{\Gamma_2} + \frac{C_3 - 1}{\Gamma_3} + \frac{C_1 C_2 - C_{1,2}}{\Gamma_1 \Gamma_2} + \frac{C_2 C_3 - C_{2,3}}{\Gamma_2 \Gamma_3} + \frac{C_1 C_3 - C_{1,3}}{\Gamma_1 \Gamma_3} \tag{3.3}$$

where the constants are defined as

$$C_1 \triangleq 2^{R_c H(\mathbf{b}_1|\mathbf{b}_2,\mathbf{b}_3)}, \tag{3.4}$$

$$C_2 \triangleq 2^{R_c H(\mathbf{b}_2|\mathbf{b}_1,\mathbf{b}_3)}, \tag{3.5}$$

$$C_3 \triangleq 2^{R_c H(\mathbf{b}_3|\mathbf{b}_1,\mathbf{b}_2)}, \tag{3.6}$$

$$C_{2,3} \triangleq 2^{R_c H(\mathbf{b}_2,\mathbf{b}_3|\mathbf{b}_1)} - 2^{R_c H(\mathbf{b}_2,\mathbf{b}_3|\mathbf{b}_1)} \left(\ln 2^{R_c H(\mathbf{b}_1|\mathbf{b}_2)} - \ln 2^{R_c H(\mathbf{b}_2|\mathbf{b}_1,\mathbf{b}_3)} \right), \tag{3.7}$$

$$C_{1,2} \triangleq 2^{R_c H(\mathbf{b}_1,\mathbf{b}_2|\mathbf{b}_3)} - 2^{R_c H(\mathbf{b}_1,\mathbf{b}_2|\mathbf{b}_3)} \left(\ln 2^{R_c H(\mathbf{b}_1|\mathbf{b}_3)} - \ln 2^{R_c H(\mathbf{b}_1|\mathbf{b}_2,\mathbf{b}_3)} \right), \tag{3.8}$$

$$C_{1,3} \triangleq 2^{R_c H(\mathbf{b}_1,\mathbf{b}_3|\mathbf{b}_2)} - 2^{R_c H(\mathbf{b}_1,\mathbf{b}_3|\mathbf{b}_2)} \left(\ln 2^{R_c H(\mathbf{b}_2|\mathbf{b}_3)} - \ln 2^{R_c H(\mathbf{b}_3|\mathbf{b}_1,\mathbf{b}_2)} \right), \tag{3.9}$$

where H represent the entropy function and R_c the spectrum efficiency of the Rayleigh fading channel, considering the channel coding scheme and the modulation multiplicity [CAM13a].

3.1.2 Optimal Power Allocation

By redistribution of power among the relays, a reduction of outage probability can be achieved. The total power of all relays represented by E_T is allocated by $\alpha_i \in [0,1]$ and $\sum_{i=1}^{3} \alpha_i = 1$ to the corresponding relay $i, \forall i$. Consequently, the average SNR can be replaced by

$$\Gamma_i = \alpha_i E_\mathrm{T}. \tag{3.10}$$

with noise variance N_0 being normalized to unity for all channels and distances $d_i, \forall i$ are assumed to be equal. Finally, Eq. (3.3) can be expressed in dependence on α_i and E_T as

$$P_\mathrm{out} \approx \frac{C_1 - 1}{E_\mathrm{T} \cdot \alpha_1} + \frac{C_2 - 1}{E_\mathrm{T} \cdot \alpha_2} + \frac{C_3 - 1}{E_\mathrm{T} \cdot \alpha_3} + \frac{C_2 \cdot C_3 - C_{2,3}}{E_\mathrm{T}^2 \cdot \alpha_2 \cdot \alpha_3} + \frac{C_1 \cdot C_2 - C_{1,2}}{E_\mathrm{T}^2 \cdot \alpha_1 \cdot \alpha_2} + \frac{C_1 \cdot C_3 - C_{1,3}}{E_\mathrm{T}^2 \cdot \alpha_1 \cdot \alpha_3}. \tag{3.11}$$

If Eq. (3.11) can be proven to be convex in $\alpha_i, \forall i$ and E_T, the outage probability can be minimized by convex optimization.

3.1.2.1 Proof of Convexity

The approximation of the outage probability can be rewritten as

$$P_\mathrm{out} \approx \sum_{n=1}^{6} c_n \cdot \alpha_1^{a_{1n}} \cdot \alpha_2^{a_{2n}} \cdot \alpha_3^{a_{3n}} \cdot E_\mathrm{T}^{a_{4n}} \tag{3.12}$$

with

n	c_n	a_{1n}	a_{2n}	a_{3n}	a_{4n}
1	$C_1 - 1$	-1	0	0	-1
2	$C_2 - 1$	0	-1	0	-1
3	$C_3 - 1$	0	0	-1	-1
4	$C_2 \cdot C_3 - C_{2,3}$	0	-1	-1	-2
5	$C_1 \cdot C_2 - C_{1,2}$	-1	-1	0	-2
6	$C_1 \cdot C_3 - C_{1,3}$	-1	0	-1	-2

If and only if $c_n > 0$ and $a_{in} \in \mathbb{R}$, then Eq. (3.12) is a *posynomial function* [BV10, Chap. 4.5]. For $(i,j,l) \in \{(1,2,3),(2,1,3),(3,1,2)\}$ and with Eq. (3.4) - Eq. (3.6) the constants are

$$c_i = C_i - 1 = 2^{R_c H(\mathbf{b}_i|\mathbf{b}_j,\mathbf{b}_l)} - 1.$$

Where $H(\mathbf{b}_i \mid \mathbf{b}_j, \mathbf{b}_l) > 0$, since the information sequences $\mathbf{b}_i$, $\mathbf{b}_j$ and $\mathbf{b}_l$ are correlated but not identical due to $(p_i, p_j, p_l) \in (0, 0.5)^3$. Consequently,

$$c_i > 0.$$

For $(k,i,j,l) \in \{(4,2,3,1),(5,1,2,3),(6,1,3,2)\}$ and with Eq. (3.7) - Eq. (3.9) the constants are

$$\begin{aligned} c_k &= C_i \cdot C_j - C_{i,j} \\ &= 2^{R_c(H(\mathbf{b}_i|\mathbf{b}_l,\mathbf{b}_j)+H(\mathbf{b}_j|\mathbf{b}_l,\mathbf{b}_i))} + 2^{R_c H(\mathbf{b}_i,\mathbf{b}_j|\mathbf{b}_l)} \left(\log 2^{R_c(H(\mathbf{b}_l|\mathbf{b}_i)-H(\mathbf{b}_i|\mathbf{b}_l,\mathbf{b}_j)} - 1\right) \\ &= 2^{R_c(H(\mathbf{b}_i,\mathbf{b}_j|\mathbf{b}_l)-H(\mathbf{b}_l|\mathbf{b}_j)+H(\mathbf{b}_j|\mathbf{b}_l,\mathbf{b}_i))} + 2^{R_c H(\mathbf{b}_i,\mathbf{b}_j|\mathbf{b}_l)} \left(\log 2^{R_c(H(\mathbf{b}_l|\mathbf{b}_i)-H(\mathbf{b}_i|\mathbf{b}_l,\mathbf{b}_j)} - 1\right) \\ &= 2^{R_c(H(\mathbf{b}_i,\mathbf{b}_j|\mathbf{b}_l)} \left(2^{R_c(H(\mathbf{b}_j|\mathbf{b}_l,\mathbf{b}_i))-H(\mathbf{b}_l|\mathbf{b}_j))} - \log 2^{R_c(H(\mathbf{b}_i|\mathbf{b}_l,\mathbf{b}_j)-H(\mathbf{b}_l|\mathbf{b}_i)} - 1\right) \end{aligned}$$

since $\mathbf{b}_i$,$\mathbf{b}_j$ and $\mathbf{b}_l$ are correlated it holds $H(\mathbf{b}_j \mid \mathbf{b}_l, \mathbf{b}_i) < H(\mathbf{b}_l \mid \mathbf{b}_j)$. It is known that $x - \log(x) > 1$ if $0 < x < 1$, as a result

$$c_k > 0.$$

Having proven Eq. (3.12) to be a *posynomial function*, the minimization of the outage probability can be performed by geometric programming. It is shown that geometric program can be transformed to a convex optimization problems [BV10, Chap. 4.5].

3.1.2.2 Simulation Settings

In the simulations two scenarios with different bit flipping probabilities are investigated

- Scenario 1 : $p_1 = 0.35 \quad p_2 = 0.01 \quad p_3 = 0.01$,
- Scenario 2 : $p_1 = 0.02 \quad p_2 = 0.10 \quad p_3 = 0.01$.

The convex optimization problem is solved with *CVX* [GB15] in geometric programming mode and the solution is verified with Monte-Carlo simulation. We assume binary phase shift keying as modulation and a channel code rate of $1/2$, thus $R_c = \frac{1}{R_M \cdot R_{cc}} = \frac{1}{\log_2 2 \cdot 1/2} = 2$. Furthermore the distance between relay and destination is $d_i = 0.5, \forall i$ and the path loss exponent $\eta = 4$.

3.1.2.3 Total Power Fixed

In this subsection we aim to minimize the outage probability while the total power is fixed. The convex optimization problem can be formulated as

$$\begin{aligned} \text{minimize} \quad & P_{\text{out}}(\alpha_1, \alpha_2, \alpha_3) \\ \text{subject to} \quad & 0 \le \alpha_i \le 1, \forall i \\ & \textstyle\sum_i \alpha_i = 1. \end{aligned} \tag{3.13}$$

Tab. 3.1 shows the scenarios where $E_T \in \{20\text{ dB}, 30\text{ dB}, 40\text{ dB}\}$. The outage probability with optimal power allocation (OPA) $P_{\text{out,OPA}}$ shows a reduction by 29.5% (scenario 1) resp. 9.6% (scenario 2) with respect to the outage probability with equal power (EP) distribution $P_{\text{out,EP}}$. Fig. 3.2 (a) shows the outage probability for $E_T \in [10\text{ dB}, 40\text{ dB}]$. A reduction of the outage probability with OPA can be observed in the whole range of E_T. The convex optimization result is verified by the Monte-Carlo simulation. Furthermore the OPA performance is close the Monte-Carlo simulation in low- and medium-SNR region. Fig. 3.2 (b) shows OPA for the E_T range. The outage probability is minimized, if more power is allocated to the relays with higher bit flipping probabilities.

$$p_i < p_j \longrightarrow \alpha_i < \alpha_j \tag{3.14}$$

With increasing E_T, the allocation converges eventually.

Table 3.1: Total power fixed

Scenario	E_T in dB	$P_{out,OPA}$	$P_{out,EP}$	Gain in %
1	20	$4.0938 \cdot 10^{-3}$	$5.7863 \cdot 10^{-3}$	29.25
	30	$4.0731 \cdot 10^{-4}$	$5.7801 \cdot 10^{-4}$	29.53
	40	$4.0718 \cdot 10^{-5}$	$5.7795 \cdot 10^{-5}$	29.55
2	20	$2.5231 \cdot 10^{-3}$	$2.7904 \cdot 10^{-3}$	9.58
	30	$2.5218 \cdot 10^{-4}$	$2.7897 \cdot 10^{-4}$	9.60
	40	$2.5216 \cdot 10^{-5}$	$2.7896 \cdot 10^{-5}$	9.61

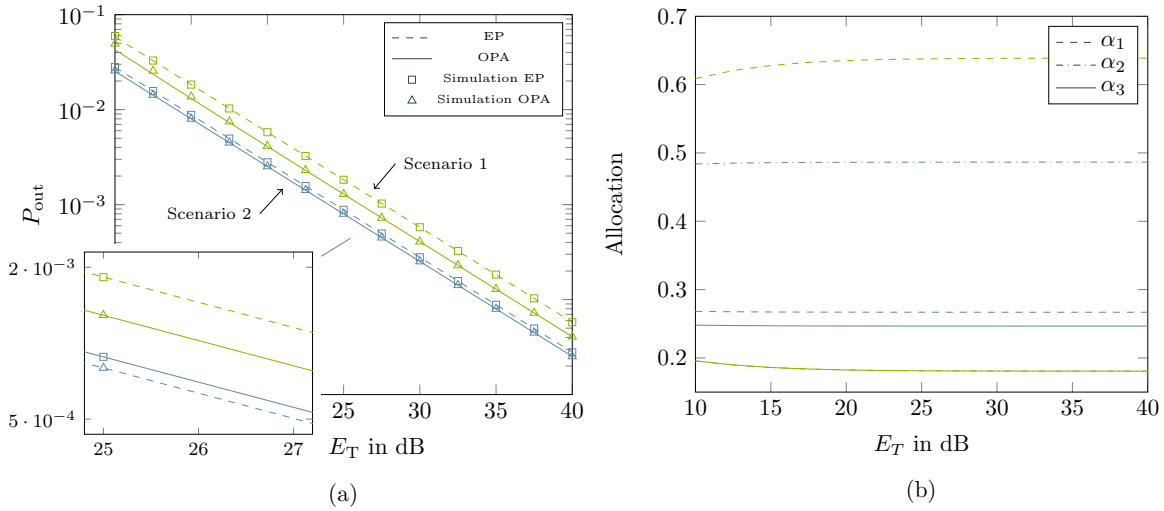

Figure 3.2: Outage probability (a) and allocation (b) with fixed total power.

3.1.2.4 Outage probability requirement fixed

In this subsection the minimum value of E_T is desired which copes with an outage probability requirement C_{out}. The minimization of E_T is achieved by OPA. We can formulate the convex optimization problem as

$$\begin{aligned} &\text{minimize} && E_T \\ &\text{subject to} && P_{out}(E_T, \alpha_1, \alpha_2, \alpha_3) - C_{out} \leq 0 \\ &&& 0 \leq \alpha_i \leq 1, \forall i \\ &&& \textstyle\sum_i \alpha_i = 1. \end{aligned} \tag{3.15}$$

Tab. 3.2 shows the two scenarios where outage probability requirement is $C_{out} \in \{10^{-3}, 10^{-4}, 10^{-5}\}$. The representative value for total power with OPA $E_{T,OPA}$ shows a reduction by 1.5 dB (scenario 1) resp. 0.45dB (scenario 2) with respect to the representative value for total power with EP distribution $E_{T,EP}$. Fig. 3.3 (a) shows E_T for outage probability requirement $C_{out} \in [10^{-5}, 10^{-1}]$ range. A gain of E_T in the hole range of outage probability requirement can be observed. The convex optimization result is verified by the Monte-Carlo simulation. Furthermore the OPA performance is close to the Monte-Carlo simulation in low- and medium-SNR region as well. Fig. 3.3 (b) shows the OPA for outage probability requirement range. With decreasing C_{out}, the allocation converges eventually.

Table 3.2: Outage probability requirement fixed

Scenario	C_{out}	$E_{\text{T,OPA}}$ in dB	$E_{\text{T,EP}}$ in dB	Gain in dB
1	10^{-3}	26.12	27.62	1.50
	10^{-4}	36.10	37.62	1.52
	10^{-5}	46.10	49.62	1.52
2	10^{-3}	24.05	24.46	0.41
	10^{-4}	34.02	34.46	0.44
	10^{-5}	43.93	44.46	0.52

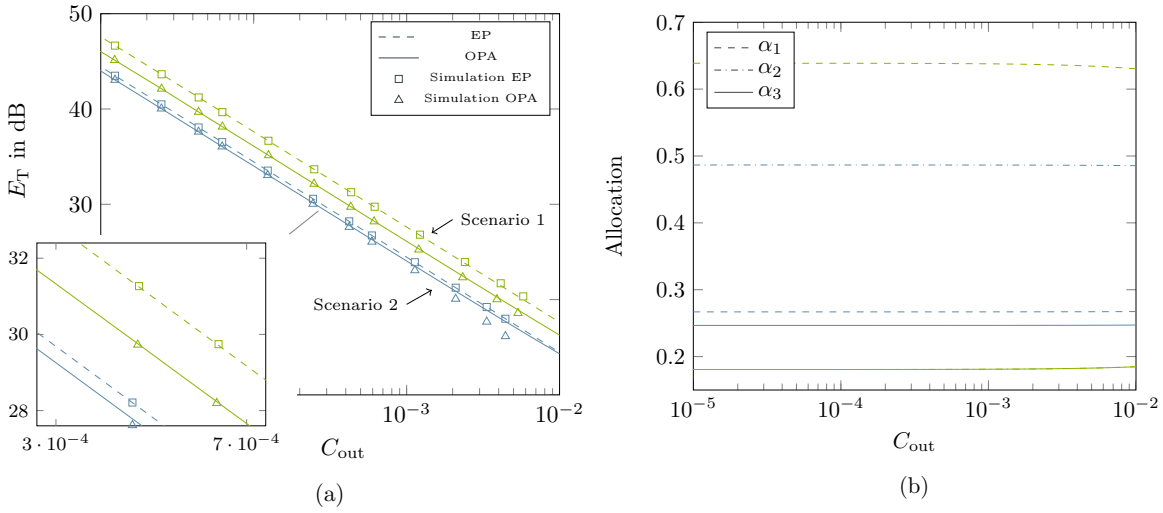

Figure 3.3: Outage probability (a) and allocation (b) with outage probability requirement fixed.

3.2 SNR Limit Based Power Allocation Algorithm

3.2.1 Motivation and Objective

We propose an algorithm for distribution of transmit power among all relays observing the same source in a wireless sensor network. Since each relay can only access erroneous observations of the source, an estimation of the underlying correct source information is performed at the destination, to which each relay reports its observations. Hence, the system follows TS 2, which can be adequately modeled by the CEO problem [BZH96]. An abstract system model is shown in Fig. 3.4. The binary source $\mathbf{S}$ is erroneously observed by the K relays, which is modeled by the random variables $\mathbf{E}_k$ which follow a Bernoulli distribution with $Pr(E_k = 1) = p_k$. At the relays, each observed data stream is encoded and transmitted over an AWGN channel to the destination, where the underlying binary sequence is estimated by jointly decoding [WMF15] all observed streams.

The task of the power allocation algorithm is to define the transmit power of each relay, so that certain requirements such as a minimum BER at the joint decoder is achieved. Since the quality of observations of each relay is described by p_k, it is intuitive to provide a power allocation scheme as a function of the BER of the different relays.

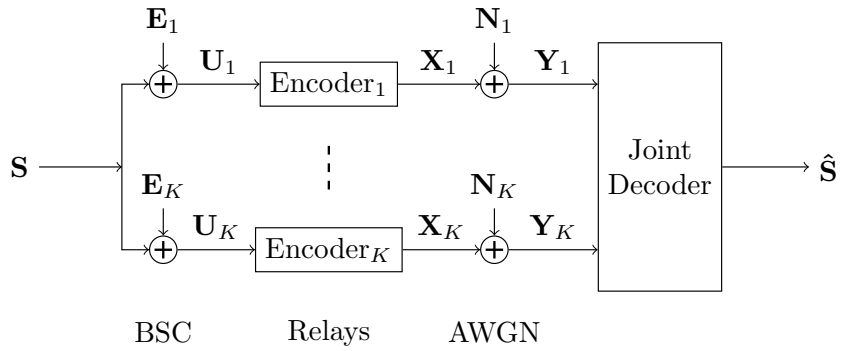

Figure 3.4: System model: Estimating a binary source observed by multiple relays.

Clearly, a good power allocation can reduce the required overall transmit power in a network, so that batteries last longer and the overall power consumption is reduced. Also, with smart resource management it is possible to reduce the outage probability of the entire network.

Four key performance indicators (KPIs) were identified that can be used to describe the performance of the joint decoder at the destination. These are

- The error floor (p_{EF}) at the destination. Due to the structure of the system model, S cannot be restored completely, but an error floor remains [WMF15]. This error floor should be educed to as low as possible.
- The SNR limit (γ_{lim}) at the destination where the BER curve reaches its error floor. Clearly, a lower γ_{lim} reduces the overall required transmit power of the system.
- The amount of active relay nodes (k_{act}). With a reduced number of relays both the transmit power and decoding quality can be improved. Furthermore, if not all relays are used for transmission, the protocol and signalling overhead in the network can be significantly reduced.
- The total transmit power (e_{T}) is the fourth KPI. Clearly, the total transmit power directly influences the total power consumption in the network and should hence be kept as low as poosible.

When looking at the definitions of the KPIs it is clear that one cannot optimize at the same time. For example, with a reduced number of relay nodes, the error floor will certainly increase. Instead, the objective is to optimize one KPI or, if possible, two KPIs and satisfy thresholds for other KPIs. We have formulated three optimization problems as follows:

1.

$$\begin{aligned} &\text{minimize} && \gamma_{\text{lim}} \\ &\text{subject to} && p_{\text{EF}} = p_{\text{all}} \\ &&& e_T = E_T \\ &&& k_{\text{act}} = K \end{aligned}$$

This objective minimizes the SNR limit by redistributing the total transmit power to all available relays. E_T represents the total transmit power budget and p_{all} the lowest possible error floor including all relays.

2.

$$\begin{aligned} &\text{minimize} && f(e_T, \gamma_{\text{lim}}) \\ &\text{subject to} && p_{\text{EF}} = p_{\text{all}} \\ &&& k_{\text{act}} = K \end{aligned}$$

In this objective, a joint metric of total transmit power and SNR limit is optimized, given that all available relays are used and hence the error floor is kept at its minimum.

3.

$$\begin{aligned} &\text{minimize} && f(k_{\text{act}}, \gamma_{\text{lim}}) \\ &\text{subject to} && p_{\text{EF}} = p_{\text{all}} \\ &&& e_T = E_T \end{aligned}$$

This metric optimizes the number of used relays. Within the proposed algorithm, the number of switched-off relays is given, and the algorithm chooses which relays to switch off. This can be extended to run the algorithm for different numbers of switched-off relays and compare the results.

3.2.2 State-of-the-Art

For the Slepian-Wolf problem in data gathering wireless sensor network (WSN), a power allocation algorithm is described in [CAM13a]. The proposed algorithm is implemented for block Rayleigh fading channels. For the CEO problem with AWGN channels, no power allocation algorithm is yet available, which is focused in this section. When looking at the typical BER curve of the proposed joint decoder in Fig. 3.5, a relatively wide ramp region appears. The simulation settings for this particular figure were set to $p = [0.17\ 0.19\ 0.03\ 0.19\ 0.13\ 0.02\ 0.06]$ but the principle behaviour is general. The ramp region, as illustrated in Fig. 3.5, can be comprehended by examining the performance of the relay decoders. The relays with low bit flipping probabilities such as relay 3 and 6 achieve arbitrarily low error rates at approximately $E_b/N_0 = -5$dB and outperform the relays 1, 2 and 4 wich suffer from large bit flipping probabilities by approximately 3dB. This phenomenon is caused by the different mutual information between one relay k and the remaining relays.

$$I(U_k; U_{k,\kappa}) = H(U_k) - H(U_k|U_{k,\kappa}) \tag{3.16}$$

where set $U_{k,\kappa} = \{U_\kappa \mid \kappa \in \mathscr{K}\backslash k\}$ and set $\mathscr{K} = \{1,2,...,K\}$. U_k is binary Bernoulli random variable such that Eq. (3.16) can be reformulated to

$$I(U_k; U_{k,\kappa}) = 1 - H(U_k|U_{k,\kappa}) \tag{3.17}$$

A causal relation between bit flipping probabilities and mutual informations holds. If

$$p_l < p_m < ... < p_n \tag{3.18}$$

with $l \neq m \neq n$ and $l,m,n \in \mathscr{K}$, the conditional entropies are relate to each other as

$$H(U_l|U_{l,\kappa}) < H(U_m|U_{m,\kappa}) < ... < H(U_n|U_{n,\kappa}). \tag{3.19}$$

Without loss of generality, we prove the above statement for $p_1 < p_2 < p_3$:

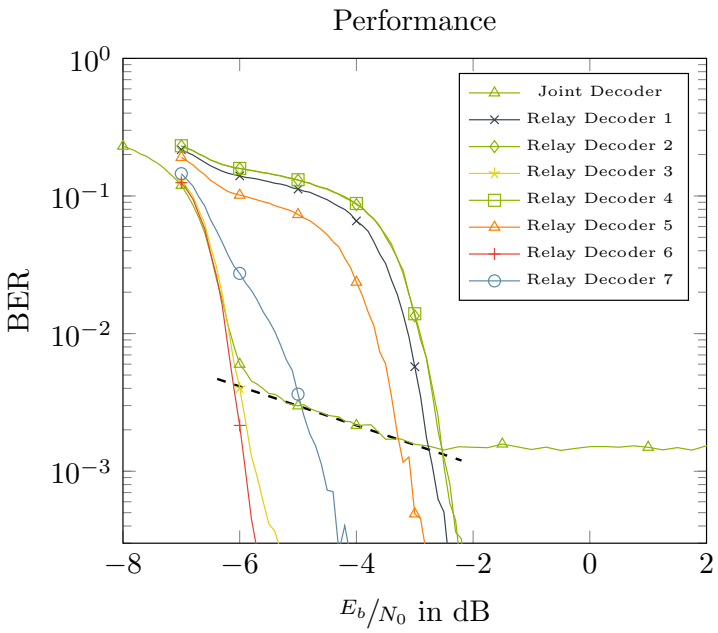

Figure 3.5: Performance of joint decoder and relay decoders.

Proof.

$$\begin{aligned} H(U_1|U_{1,\{2,3\}}) &= H(U_1,U_2,U_3) - H(U_2|U_3) - H(U_3) \\ &= H(U_1,U_2,U_3) - H(p_2+p_3-2\cdot p_2\cdot p_3) - 1 \\ &> H(U_1,U_2,U_3) - H(p_1+p_3-2\cdot p_1\cdot p_3) - 1 = H(U_2|U_{2,\{1,3\}}) \\ &> H(U_1,U_2,U_3) - H(p_1+p_2-2\cdot p_1\cdot p_2) - 1 = H(U_3|U_{3,\{1,2\}}) \end{aligned}$$

□

As a consequence, the mutual information can be ordered according to Eq. (3.17) as

$$I(U_l;U_{l,\kappa}) > I(U_m;U_{m,\kappa}) > \ldots > I(U_n;U_{n,\kappa}). \tag{3.20}$$

This implies, that any relay decoder with low bit flipping probability benefits to a greater extent from the information exchange executed via the global iteration (GI). It therefore achieves an arbitrarily low error rate, despite the fact that the AWGN channel is suffering from significant noise. A relay decoder with a high bit flipping probability depends more on reliable information from the relay transmitted over the AWGN channel since the information exchange from the GI is not as beneficial. Finally, at $\gamma_{\text{lim}} = -2$ dB all relays can be decoded correctly and hence the decoder reaches its error floor.

Hence, in order to lower γ_{lim}, it is necessary that the relay decoders for the high bit flipping probabilities are decoded at a lower SNR. Naturally, this can be achieved by distributing more power to these relays. On the other hand, relays with low bit flipping probability can transmit with a lower transmit power, since they benefit more from the other transmitting relays. In the end, the SNR limits for each relay decoder should fall together in order to reduce the overall SNR limit as much as possible. This is illustrated in Fig. 3.6, where the SNR limits per relay decoder are depicted as vertical dashed lines.

Fig. 3.7 illustrates the power distribution used in Fig. 3.5, i.e. equal power allocation, which is depicted by equally sized blocks for each relay also refereed to as the reference case. In order to describe different power allocations, we introduce the variable power allocation variable α_k which describes the ratio of the overall transmit power that is transmitted by the k^{th} relay. Hence, the transmit energy of the k^{th} relay is given by

$$E_k = \alpha_k E_T / K \tag{3.21}$$

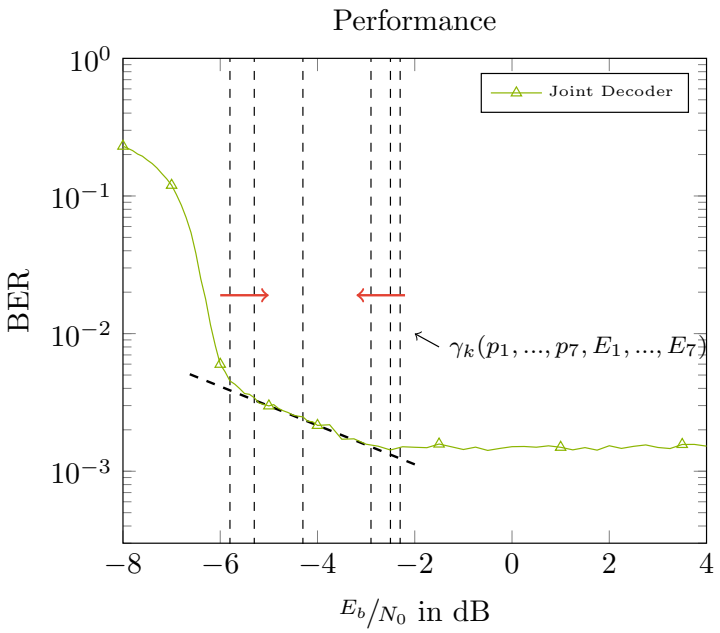

Figure 3.6: Performance of joint decoder and SNR limits of relay decoders.

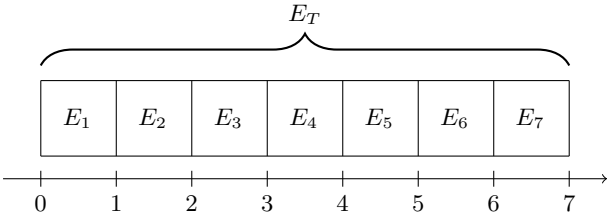

Figure 3.7: Equal transmit power distribution among relays.

where E_T is the total available transmit energy and

$$\sum_k \alpha_k = K. \tag{3.22}$$

For a given set of bit flipping probabilities, the SNR limits for the relay decoders are a function of $\{\alpha_k\}$. With the knowledge of this function, the power allocation can be optimized. However, the analytical derivation of this expression remains an open problem up to now and the following algorithm is based on a numerical evaluation.

3.2.3 Implemented Power Allocation Algorithm

Algorithm 1 optimizes the transmit power for each relay such that the SNR limits of each relay decoder align at one common SNR. Initially, it equally distributes the available transmit power to all relays and runs the joint decoder (JD) at the destination. Then, for each relay decoder it is evaluated at which SNR $\gamma_{k,T}$ it reaches a given BER T_{BER}. This information is then translated into an adaptation of the allocated transmit power for each relay by comparing $\gamma_{k,T}$ to the mean of all SNR limits. However, the maximum change in the transmit power for each relay and iteration is given by the parameter β. β adapts to the improvement of the relay decoders and finally reaches a small value such that the convergence of the algorithm is ensured. Finally, the parameter ε describes the required accuracy of the algorithm, i.e. how close the SNR limits for the relay decoders should be to each other and hence provides a trade-off between accuracy and complexity.

Algorithm 1: Power allocation

Input: ε: tolerated range; β: redistribution maximum; M: maximum iteration;
K: number of relays; E_T: total transmit power
Output: α_k: power distribution
Initialization: $\alpha_k(1) = {}^1/_K, \forall k$;
for $m = 1$ **to** M **do**
  Run JD with $E_k = \alpha_k(m) \cdot E_T, \forall k$ in SNR range;
  Output BER_k for relay decoder;
  Calculate $\gamma_{k,\mathrm{T}} = \gamma_k(\mathrm{BER}_k = T_{\mathrm{BER}})$;
  Calculate $\gamma_{\mathrm{dif}} = \min_k(T_{\gamma_k}) - \max_k(T_{\gamma_k})$;
  if $\gamma_{dif} \leq \varepsilon$ **then**
    $\alpha_k^{\mathrm{final}} = \alpha_k(m), \forall k$;
    Exit **for**;
  else
    $\alpha_k(m+1) = \alpha_k(m) - \beta \cdot \frac{\gamma_{k,\mathrm{T}} - \mathbb{E}(\gamma_{,\mathrm{T}})}{\mathbb{E}(\gamma_{,\mathrm{T}})}, \forall k$;
  end
  if m=M **then**
    $\alpha_k^{\mathrm{final}} = \alpha_k(M), \forall k$;
  end
end

3.2.4 Simulation Results

In this section, the performance of the power allocation algorithm and the resulting decoding performance at the destination are evaluated. Simulations are carried out for three and seven relays with bit flipping probabilities given in Tab. 3.3. However, for the three-relay case it only makes sense to optimize for objective one. The resulting optimal power allocations are given as the third column in this table.

Table 3.3: Simulation Settings

	Bit flipping probabilities p	Objectives	power distribution α
3 Relays	0.11 0.17 0.04	1.	0.987 1.119 0.894
7 Relays	0.17 0.19 0.03 0.19 0.13 0.02 0.06	1.	1.234 1.308 0.623 1.317 1.125 0.575 0.815
		2.	0.896 0.942 0.537 0.926 0.812 0.497 0.637
	0.17 ~~0.19~~ 0.03 ~~0.19~~ 0.13 0.02 0.06	3.	2.306 0.872 1.880 0.773 1.167

1. Objective

$$\begin{array}{ll} \text{minimize} & \gamma_{\mathrm{lim}} \\ \text{subject to} & p_{\mathrm{EF}} = p_{\mathrm{all}} \\ & e_{\mathrm{T}} = E_{\mathrm{T}} \\ & k_{\mathrm{act}} = K \end{array}$$

Fig. 3.8 shows the power redistribution among seven relays (cf. Tab 3.3). The allocation assigns more power to relays with high bit flipping probabilities. Relays with low bit flippling probabilities are allocated less power.

For the three-relay case, the behaviour is similar, as shown in Tab. 3.3. Fig. 3.9 shows the performance of the joint decoder when using three relays. Obviously, the SNR limits for the relay decoders overlap and hence the ramp region in the BER curve is shorter. However, the ramp region starts at higher SNR compared to the equal power distribution case and in overall, the performance of BER curve is not strongly influenced by the different power allocation.

For seven relays a strong alignment of relay decoder SNR limits is shown in Fig. 3.10 (b). More power is assigned to the relays with higher bit flipping probabilities which improves the performance of corresponding decoders and

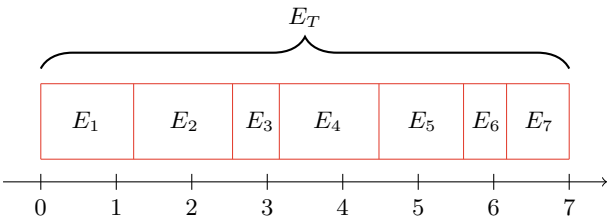

Figure 3.8: Redistributed transmit power among relays by means to fulfil first objective.

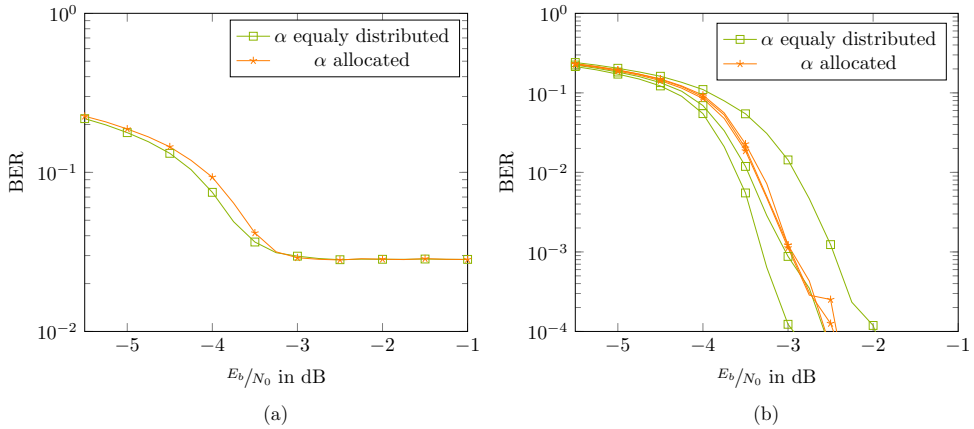

Figure 3.9: Three relays - performance of joint decoder (a) and relay decoders (b) for first objective.

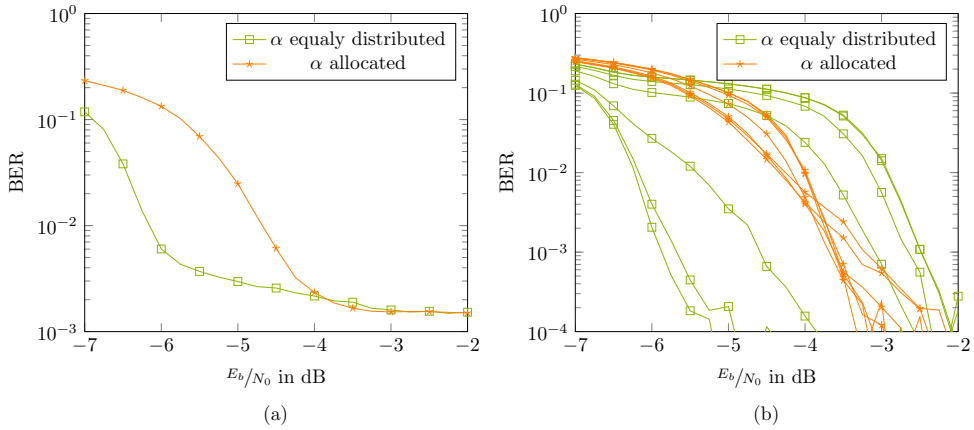

Figure 3.10: Seven relays - performance of joint decoder (a) and relay decoders (b) for first objective.

consequently a significant improvement of γ_{lim} can be observed. As a result the BER curve shows a smaller ramp region in Fig. 3.10 (a) compared to the reference case. However relay decoders with low bit flipping probabilities experience a significant drop in performance and thus, a shift of the waterfall region towards a higher SNR value appears.

2. Objective

$$\begin{array}{ll} \text{minimize} & f(e_{\text{T}}, \gamma_{\text{lim}}) \\ \text{subject to} & p_{\text{EF}} = p_{\text{all}} \\ & k_{\text{act}} = K \end{array}$$

Fig. 3.11 shows the power redistribution among seven relays subject to a reduction of total transmit power by 25% (cf. Tab 3.3) compared to the reference case.

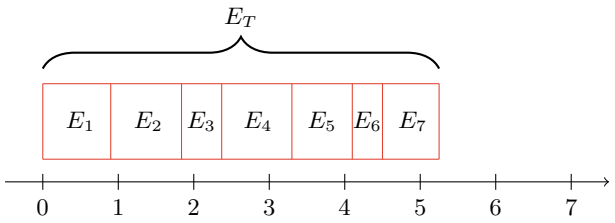

Figure 3.11: Redistributed transmit power among relays by means to fulfil second objective.

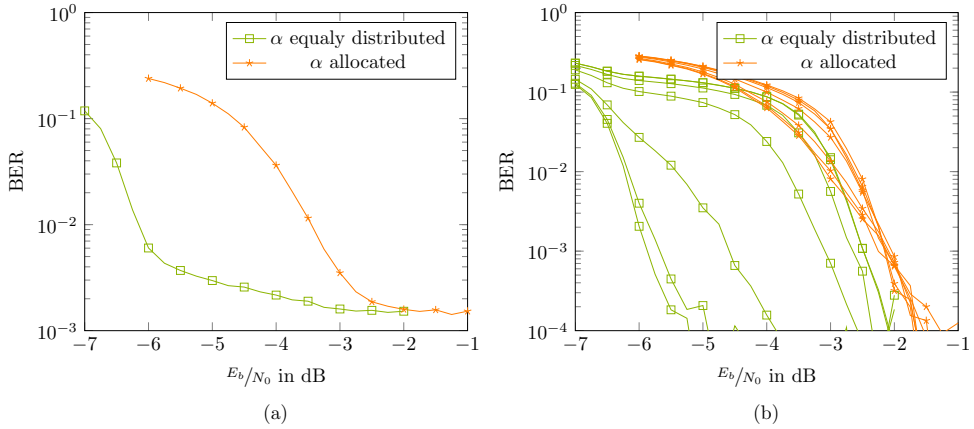

Figure 3.12: Seven relays - performance of joint decoder (a) and relay decoders (b) for second objective.

Fig. 3.12 (b) shows a strong alignment of relay decoder SNR limits for power redistribution among the seven relays. Despite the reduction of total transmit power the SNR limit can remain the same compared to the reference case. As a result the BER curve hits the error floor at the same SNR value as the reference case, depicted in Fig. 3.12 (a). Moreover the BER curve shows a smaller ramp region due to the strong alignment of relay decoder SNR limits. However, a significant loss in the waterfall region appears due to the reduced transmit power of all relays.

3. Objective

$$\begin{array}{ll} \text{minimize} & f(k_{\text{act}}, \gamma_{\text{lim}}) \\ \text{subject to} & p_{\text{EF}} = p_{\text{all}} \\ & e_{\text{T}} = E_{\text{T}} \end{array}$$

Fig. 3.13 shows the power redistribution among all relays subject to a reduction of active relays by two (cf. Tab 3.3) compared to the reference case. Since two relays are no longer required to use power resources, more transmit power is allocated to the remaining relays.

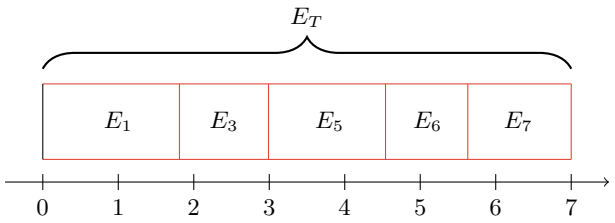

Figure 3.13: Redistributed transmit power among relays by means to fulfill third objective.

A tremendous reduction of γ_{lim} is achieved by the redistribution of the power and reducing the active relays. Furthermore the relay decoder SNR limits can be aligned. Consequently the ramp region is reduced as shown in Fig. 3.14 (a) compared to the reference case. The BER curve hits the possible error floor for five relays at a lower SNR limit compared to the reference case. However, the error floor of five relays is higher compared to the error floor of seven relays [WMF15].

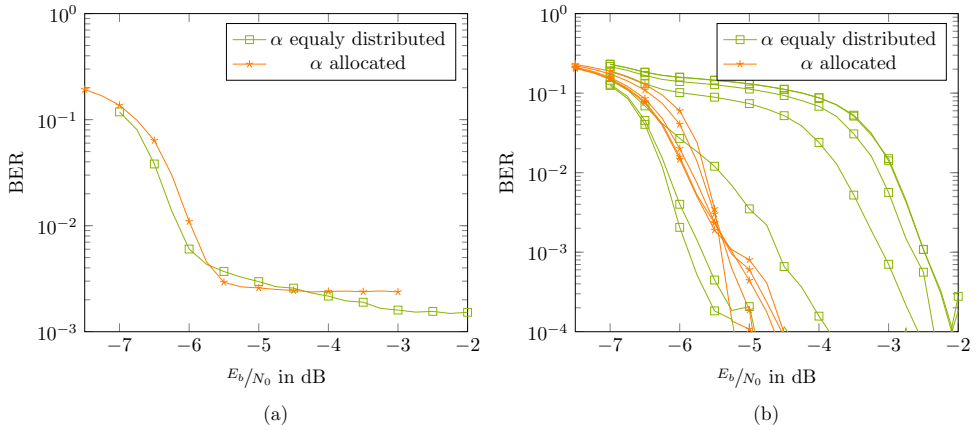

Figure 3.14: Seven relays - performance of joint decoder (a) and relay decoders (b) for third objective.

3.2.5 Summary

A power allocation algorithm has been described that aims to equalize the SNR limits for each relay decoder, such that the ramp region of the joint decoder can be removed or reduced. The proposed algorithm shows significant improvements in the SNR limit for the relay decoders, and the BER curve of the joint decoder qualitatively follows as expected. However, no significant improvements for the BER of the joint decoder could be achieved with the proposed approach.

4. Power Allocation for Orthogonal Multiple Access Relay Channel Allowing Intra-link Errors

4.1 Motivation and Objective

Decode-and-forward (DF) [NHH04] is one of the classical relaying strategies applied in cooperative wireless networks. The signals transmitted from source nodes are able to be re-generated in the DF strategies such that the noise propagation can be avoided. Quite recently, several resource allocation problems for DF-based orthogonal MARC systems have been investigated. For example, in [EZL+10] and [SAK12], the sum rates of the DF-based orthogonal MARC systems are maximized at the destination by optimally allocating the power for the different nodes and carriers with the total and individual power constraints, respectively. In [AB14], weighted sum rate maximization (WSRM) is studied for a two-user DF-based MARC system with using orthogonal frequency division multiple access (OFDMA).

However, it has been found in [LZA+14] that even the estimates are incorrectly decoded at the relay, the forwarded erroneous estimates are still helpful for the reconstruction of the information sequences sent from the source nodes at the destination. Moreover, it is shown in [LZM14], that the outage performance is improved by forwarding the incorrectly decoded estimates, especially when one of the source nodes is quite far away from both the relay and destination.

The main contributions of this section are summarized as follows: A power minimization problem subject to lossy rate constraints is formulated for MARC. Successive convex approximation (SCA) [MW78] algorithm is used for solving the non-convex problem. Furthermore, convergence of the algorithm is justified.

4.2 System Model

Block diagram of an orthogonal MARC is shown in Fig. 4.1, where two source nodes S_1 and S_2 are communicating with a common destination D with the assist of a relay node R. It is assumed that all the nodes are equipped with single antenna, and R works in a half-duplex mode. The K-bit length i.i.d. binary information sequence generated from S_1 and S_2 are denoted as $\mathbf{u}_1 = \{u_1(i)\}_{i=1}^{K}$ and $\mathbf{u}_2 = \{u_2(i)\}_{i=1}^{K}$. There are three time slots in one transmission cycle. In the first two time slots, S_1 and S_2 encode $\mathbf{u}_1$ and $\mathbf{u}_2$, and broadcast the coded sequence $\mathbf{x}_1 = \{x_1(i)\}_{i=1}^{N_1}$ and $\mathbf{x}_2 = \{x_2(i)\}_{i=1}^{N_2}$ to both R and D, respectively.

In the third time slot, R first tries to reconstruct $\mathbf{u}_1$ and $\mathbf{u}_2$ that transmitted from S_1 and S_2, of which the estimates are denoted as $\tilde{\mathbf{u}}_1$ and $\tilde{\mathbf{u}}_2$, respectively. Different from the conventional DF protocol, R always combines the two estimates as $\mathbf{u_r} = \tilde{\mathbf{u}}_1 \oplus \tilde{\mathbf{u}}_2$ in the system considered even though $\tilde{\mathbf{u}}_1$ and $\tilde{\mathbf{u}}_2$ may contain errors. Here $\oplus$ indicates modulus-2 addition. $\mathbf{u}_r$ is then interleaved, re-encoded into coded sequence $\mathbf{x}_r = \{x_r(i)\}_{i=1}^{N_r}$, and forwarded to D. Finally, after receiving signals from S_1, S_2 and R, joint decoding is performed at D to retrieve the original information sequences $\mathbf{u}_1$ and $\mathbf{u}_2$.

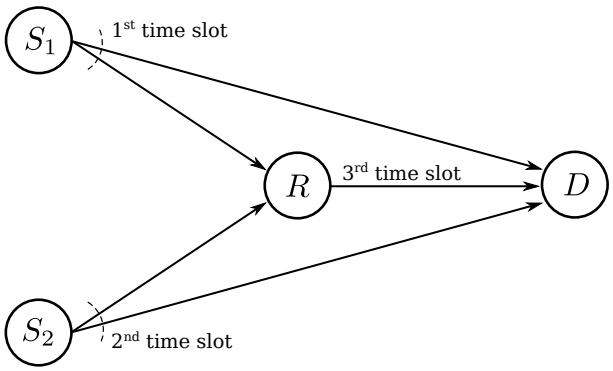

Figure 4.1: The block diagram of orthogonal MARC.

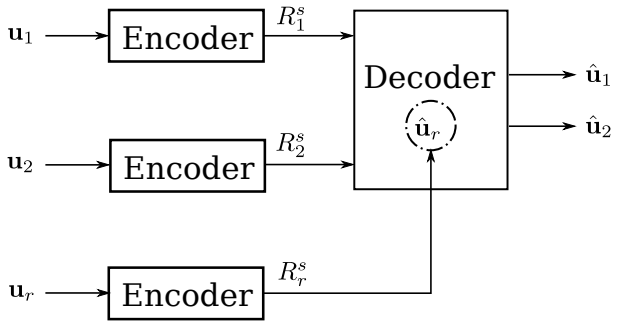

Figure 4.2: Abstract model for lossless source coding of $\mathbf{u}_1$ and $\mathbf{u}_2$ with the help of $\mathbf{u}_r$.

The code rate of S_1, S_2 and R are defined as $R_1 = K/N_1$, $R_2 = K/N_2$ and $R_r = K/N_r$, respectively. Let $L_{i,j},\ i \in \{S_1, S_2, R\},\ j \in \{R, D\},\ i \neq j$, denote the link between node i and j. The received signal of $L_{i,j}$ can be expressed as

$$\mathbf{y}_{i,j} = \sqrt{G_{i,j}} \cdot \sqrt{P_i} \cdot \mathbf{x}_i + \mathbf{n}_{i,j}, \tag{4.1}$$

where $G_{i,j}$ is the geometric-gain of $L_{i,j}$, P_i is the average transmit power at node i, and $\mathbf{n}_{i,j}$ is the vector of independent zero-mean complex AWGN with variance $\sigma_{i,j}^2 = N_0/2$ per dimension. Let $d_{i,j}$ denote the distance of $L_{i,j}$ and $G_{S_1,D}$ being normalized to unity. Then, $G_{i,j}$ can be defined as

$$G_{i,j} \triangleq \left(\frac{d_{S_1,D}}{d_{i,j}} \right)^l, \tag{4.2}$$

where l is the pathloss exponent.

4.3 Conditions for Reliable Transmission

In this section, we investigate the conditions that guarantee reliable transmission from S_1 and S_2 to D. First we look at the transmission from S_1 to R. As described above, errors are allowed at R after decoding. According to Shannon's lossy source-channel separation theorem [Sha59; VFC+14], $\mathbf{u}_1$ can be transmitted from S_1 to R with a distortion level $\mathscr{D}_1$ if the following inequality is satisfied:

$$R(\mathscr{D}_1) \cdot R_1 \leq C(\frac{G_{S_1,R} P_1}{N_0}), \tag{4.3}$$

where $R(\mathscr{D}_1)$ and $C(x) = \log_2(1+x)$ are the rate-distortion function and the Gaussian capacity function, respectively. With hamming distortion measure, $\mathscr{D}_1 = \frac{1}{K} \sum_{i=1}^{K} d(u_1(i), \tilde{u}_1(i))$, where

$$d(u_1(i), \tilde{u}_1(i)) = \begin{cases} 1, & \text{if} \quad u_1(i) \neq \tilde{u}_1(i), \\ 0, & \text{if} \quad u_1(i) = \tilde{u}_1(i), \end{cases} \tag{4.4}$$

and $R(\mathscr{D}_1) = 1 - H_2(\mathscr{D}_1)$, where $H_2(x) = -x \log_2 x - (1-x)\log_2(1-x)$ is the binary entropy function. In the similar way, the condition for transmitting $\mathbf{u}_2$ from S_2 to R with a distortion level $\mathscr{D}_2$ is

$$R(\mathscr{D}_2) \cdot R_2 \leq C(\frac{G_{S_2,R} P_2}{N_0}). \tag{4.5}$$

Next we consider the transmission of $\mathbf{u}_1$, $\mathbf{u}_2$ and $\mathbf{u}_r$ to D from S_1, S_2 and R, respectively. Note that $\mathbf{u}_r$ is not to be recovered at D, in other words, $\mathbf{u}_r$ serve as a helper in recovering $\mathbf{u}_1$ and $\mathbf{u}_2$ at D, as shown in Fig. 4.2. This problem falls exactly into the category of lossless source coding with one helper. Assume $\mathbf{u}_1$, $\mathbf{u}_2$ and $\mathbf{u}_r$ are first described with rates R_1^s, R_2^s and R_r^s, respectively. According to the theorem in [GK11, Theorem 10.4], the admissible rate region is specified as

$$\begin{cases} R_1^s & \geq & H(\mathbf{u}_1 | \mathbf{u}_2, \hat{\mathbf{u}}_r), \\ R_2^s & \geq & H(\mathbf{u}_2 | \mathbf{u}_1, \hat{\mathbf{u}}_r), \\ R_1^s + R_2^s & \geq & H(\mathbf{u}_1, \mathbf{u}_2 | \hat{\mathbf{u}}_r), \\ R_r^s & \geq & I(\mathbf{u}_r; \hat{\mathbf{u}}_r), \end{cases} \tag{4.6}$$

where $\hat{\mathbf{u}}_r$ is the estimate of $\mathbf{u}_r$ at the final output, as shown in Fig. 4.2. Let $\mathscr{D}_3$ denote the hamming distortion between $\hat{\mathbf{u}}_r$ and $\mathbf{u}_r$. By using the similar approach as in [LZM14], (4.6) can be further expressed as

$$\begin{cases} R_1^s & \geq & H_2(\mathscr{D}_1 * \mathscr{D}_2 * \mathscr{D}_3), \\ R_2^s & \geq & H_2(\mathscr{D}_1 * \mathscr{D}_2 * \mathscr{D}_3), \\ R_1^s + R_2^s & \geq & 1 + H_2(\mathscr{D}_1 * \mathscr{D}_2 * \mathscr{D}_3), \\ R_r^s & \geq & 1 - H_2(\mathscr{D}_3), \end{cases} \tag{4.7}$$

where $x * y = x(1-y) + (1-x)y$ is the binary convolution.

On the other hand, according to Shannon's separation theorem, if the total information transmission rates over the three independent channels satisfy

$$\begin{cases} R_1^s R_1 & \leq & C(\frac{G_{S_1,D}P_1}{N_0}), \\ R_2^s R_2 & \leq & C(\frac{G_{S_2,D}P_2}{N_0}), \\ R_r^s R_r & \leq & C(\frac{G_{R,D}P_r}{N_0}), \end{cases} \tag{4.8}$$

the message error probability can be made arbitrarily small.

In order to achieve reliable transmission of $\mathbf{u}_1$ and $\mathbf{u}_2$, the conditions shown in (4.3), (4.5), (4.7) and (4.8) should be satisfied simultaneously. These conditions are reformulated and summarized as

$$\begin{cases} 1 - H_2(\mathscr{D}_1) & \leq & \frac{1}{R_1} C(\frac{G_{S_1,R}P_1}{N_0}), \\ 1 - H_2(\mathscr{D}_2) & \leq & \frac{1}{R_2} C(\frac{G_{S_2,R}P_2}{N_0}), \\ 1 - H_2(\mathscr{D}_3) & \leq & \frac{1}{R_r} C(\frac{G_{R,D}P_r}{N_0}), \\ H_2(\mathscr{D}_1 * \mathscr{D}_2 * \mathscr{D}_3) & \leq & \frac{1}{R_1} C(\frac{G_{S_1,D}P_1}{N_0}), \\ H_2(\mathscr{D}_1 * \mathscr{D}_2 * \mathscr{D}_3) & \leq & \frac{1}{R_2} C(\frac{G_{S_2,D}P_2}{N_0}), \\ 1 + H_2(\mathscr{D}_1 * \mathscr{D}_2 * \mathscr{D}_3) & \leq & \frac{1}{R_1} C(\frac{G_{S_1,D}P_1}{N_0}) + \frac{1}{R_2} C(\frac{G_{S_2,D}P_2}{N_0}). \end{cases} \tag{4.9}$$

4.4 Power Minimization with Rate Constraints

In this section, a power minimization problem with the conditions for reliable transmission is derived. Then, SCA is applied for solving the non-convex problem. The power minimization problem with constraints shown in (4.9) is expressed as

$$\begin{aligned} \underset{\mathbf{P},\mathbf{D}}{\text{minimize}} \quad & P_1 + P_2 + P_r \\ \text{subject to} \quad & 1 - H_2(\mathscr{D}_1) \leq \tfrac{1}{R_1} C(\tfrac{G_{S_1,R}P_1}{N_0}), \text{ (i)} \\ & 1 - H_2(\mathscr{D}_2) \leq \tfrac{1}{R_2} C(\tfrac{G_{S_2,R}P_2}{N_0}), \text{ (ii)} \\ & 1 - H_2(\mathscr{D}_3) \leq \tfrac{1}{R_r} C(\tfrac{G_{R,D}P_r}{N_0}), \text{ (iii)} \\ & H_2(\mathscr{D}_1 * \mathscr{D}_2 * \mathscr{D}_3) \leq \tfrac{1}{R_1} C(\tfrac{G_{S_1,D}P_1}{N_0}), \text{ (iv)} \\ & H_2(\mathscr{D}_1 * \mathscr{D}_2 * \mathscr{D}_3) \leq \tfrac{1}{R_2} C(\tfrac{G_{S_2,D}P_2}{N_0}), \text{ (v)} \\ & 1 + H_2(\mathscr{D}_1 * \mathscr{D}_2 * \mathscr{D}_3) \leq \\ & \tfrac{1}{R_1} C(\tfrac{G_{S_1,D}P_1}{N_0}) + \tfrac{1}{R_2} C(\tfrac{G_{S_2,D}P_2}{N_0}) \text{ (vi)}, \end{aligned} \tag{4.10}$$

where $\mathbf{P} = [P_1, P_2, P_r]$ and $\mathbf{D} = [\mathscr{D}_1, \mathscr{D}_2, \mathscr{D}_3]$.

4.4.1 Successive Convex Approximation

In the following, we derive an SCA for the non-convex power minimization problem shown in (4.10). It is well known that binary entropy function $H_2 : [0, 0.5] \to [0, 1]$ is concave and increasing when its argument is in $[0, 0.5]$. Furthermore, logarithm is also a concave function and therefore, constraints (i-iii) are convex constraints. Let $f(\mathscr{D}_1, \mathscr{D}_2, \mathscr{D}_3) : [0, 0.5]^3 \to [0, 0.5]$ denote the binary convolution $\mathscr{D}_1 * \mathscr{D}_2 * \mathscr{D}_3$. Calculating the Hessian of f, it can be shown that f is a concave function. Using a vector composition result from [BV04, Chpt. 3.], it is directly seen

that $H_2(f(\mathscr{D}_1,\mathscr{D}_2,\mathscr{D}_3))$ is a concave function. Therefore, it needs to be approximated by its convex upper bound, i.e., linear function. A local linear approximation of $f(\mathscr{D}_1,\mathscr{D}_2,\mathscr{D}_3)$ at a point $(\hat{\mathscr{D}}_1,\hat{\mathscr{D}}_2,\hat{\mathscr{D}}_3)$ is derived as

$$\begin{aligned}&\hat{f}(\mathscr{D}_1,\mathscr{D}_2,\mathscr{D}_3)=\\&f(\hat{\mathscr{D}}_1,\hat{\mathscr{D}}_2,\hat{\mathscr{D}}_3)+\sum_{k=1}^{3}\frac{\partial f(\hat{\mathscr{D}}_1,\hat{\mathscr{D}}_2,\hat{\mathscr{D}}_3)}{\partial \mathscr{D}_k}(\mathscr{D}_k-\hat{\mathscr{D}}_k).\end{aligned} \tag{4.11}$$

Due to the concavity of f, it holds that $\hat{f}(\mathscr{D}_1,\mathscr{D}_2,\mathscr{D}_3)\geq f(\mathscr{D}_1,\mathscr{D}_2,\mathscr{D}_3)$. Let $\hat{f}(\mathscr{D}_1,\mathscr{D}_2,\mathscr{D}_3)=\tilde{\mathscr{D}}$. Similarly, we can approximate $H_2(\tilde{\mathscr{D}})$ at a point $\hat{\mathscr{D}}$ by $\hat{H}_2(\tilde{\mathscr{D}})$ as

$$\hat{H}_2(\tilde{\mathscr{D}})=H_2(\hat{\mathscr{D}})+\log_2(\frac{1-\hat{\mathscr{D}}}{\hat{\mathscr{D}}})(\tilde{\mathscr{D}}-\hat{\mathscr{D}}). \tag{4.12}$$

Now it holds that $\hat{H}_2(\tilde{\mathscr{D}})\geq H_2(\tilde{\mathscr{D}})$. Using the property that $H_2(\tilde{\mathscr{D}})$ is an increasing function and using the original notation of $\hat{f}(\mathscr{D}_1,\mathscr{D}_2,\mathscr{D}_3)$, it also holds that

$$\hat{H}_2(\hat{f}(\mathscr{D}_1,\mathscr{D}_2,\mathscr{D}_3))\geq H_2(f(\mathscr{D}_1,\mathscr{D}_2,\mathscr{D}_3)). \tag{4.13}$$

The approximated optimization problem is written as

$$\begin{aligned}\underset{\mathbf{P},\mathbf{D}}{\text{minimize}}\quad & P_1+P_2+P_r\\ \text{subject to}\quad & 1-H_2(\mathscr{D}_1)\leq\tfrac{1}{R_1}C(\tfrac{G_{S_1,R}P_1}{N_0}),\\ & 1-H_2(\mathscr{D}_2)\leq\tfrac{1}{R_2}C(\tfrac{G_{S_2,R}P_2}{N_0}),\\ & 1-H_2(\mathscr{D}_3)\leq\tfrac{1}{R_r}C(\tfrac{G_{R,D}P_r}{N_0}),\\ & \hat{H}_2(\hat{f}(\mathscr{D}_1,\mathscr{D}_2,\mathscr{D}_3))\leq\tfrac{1}{R_1}C(\tfrac{G_{S_1,D}P_1}{N_0}),\\ & \hat{H}_2(\hat{f}(\mathscr{D}_1,\mathscr{D}_2,\mathscr{D}_3))\leq\tfrac{1}{R_2}C(\tfrac{G_{S_2,D}P_2}{N_0}),\\ & 1+\hat{H}_2(\hat{f}(\mathscr{D}_1,\mathscr{D}_2,\mathscr{D}_3))\leq\\ & \tfrac{1}{R_1}C(\tfrac{G_{S_1,D}P_1}{N_0})+\tfrac{1}{R_2}C(\tfrac{G_{S_2,D}P_2}{N_0}),\end{aligned} \tag{4.14}$$

which is a convex problem and can be efficiently solved using standard optimization tools, e.g., interior-point methods [BV04]. It is worth noticing that due to the inequality (4.13), the solution of (4.14) satisfies the constraints of the original problem (4.10).

The SCA algorithm starts by a feasible initialization $\hat{\mathscr{D}}_k=\hat{\mathscr{D}}_k^{(0)},\forall k$. After this, (4.14) is solved yielding a solution $\mathscr{D}_k^{(*)}$ which is used as a new point for the linear approximation. The procedure is repeated until convergence. **Algorithm** 2 provides the description for the SCA algorithm. The inequality (4.13) states that the linear approximation is always above the approximated function. Therefore, this algorithm is guaranteed to monotonically converge to a local optimum of the original problem [MW78].

Algorithm 2: Successive convex approximation algorithm.

1: Set $\hat{\mathscr{D}}_k=\hat{\mathscr{D}}_k^{(0)},\forall k$.
2: **repeat**
3: Solve Eq. (4.14).
4: Update $\hat{\mathscr{D}}_k=\mathscr{D}_k^{(*)},\forall k$.
5: **until** Convergence.

4.5 Simulation Results

In this section, we present the numerical results to demonstrate the impact of power allocation in RESCUE system and illustrate its superiority compared with lossless DF in terms of total power consumption. The pathloss exponent l is empirically set at 3.52 according to [YG11]. The simulation setup is defined in Fig. 4.3. We will place the source and destination nodes into the Euclidean space and move the relay along the horizontal axis.

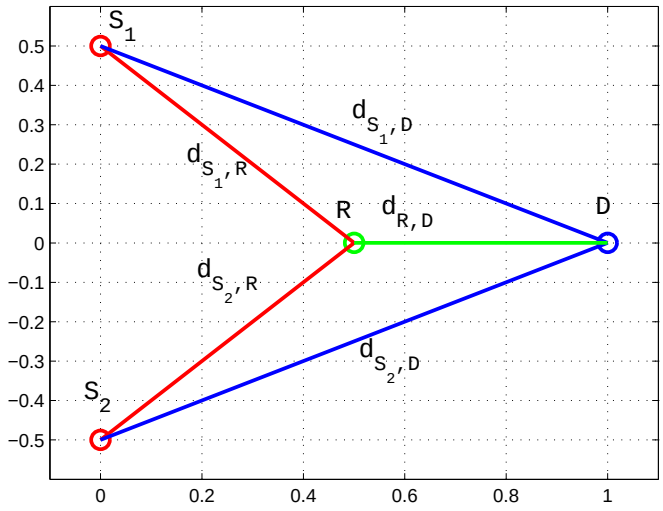

Figure 4.3: Simulation setup.

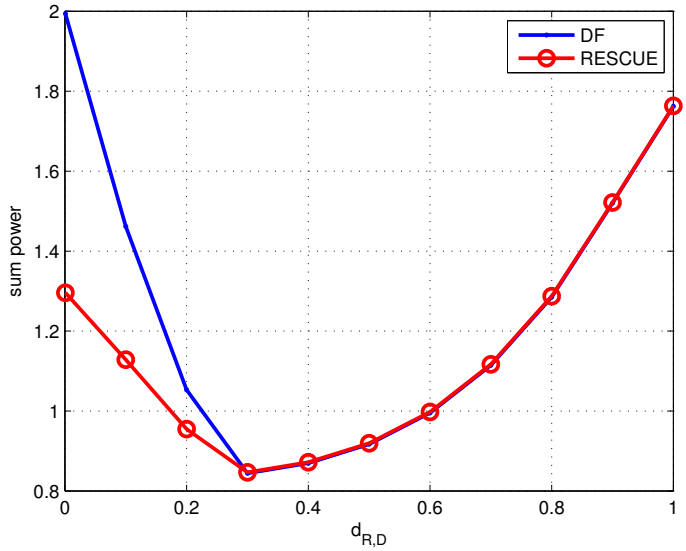

Figure 4.4: Sum power versus relay location.

As a first simulation example, we consider symmetric scenario where the nodes are placed at the points $S_1 = (0, 0.5)$, $S_2 = (0, -0.5)$ and $D = (1, 0)$, i.e., $d_{S1,R} = d_{S2,R}$ and $d_{S1,D} = d_{S2,D}$. Sum power versus d_R, D is plotted in Fig. 4.4. It can be seen that the RESCUE scheme performs better in terms of the total power consumption when the relay is close to the destination.

In the second example, the nodes are placed at the points $S_1 = (0, 1)$, $S_2 = (0, -1)$ and $D = (1, 0)$. The results are shown in Fig. 4.5. The range where the RESCUE scheme is superior is larger compared to the case presented in Fig. 4.4 because the sources are further away from the relay and the destination.

The third example is an asymmetric case where the nodes are at the points $S_1 = (0, 1)$, $S_2 = (0, -2)$ and $D = (1, 0)$. The results are shown in Fig. 4.6. It can be seen that the RESCUE scheme is superior compared to the lossless case through the whole range of relay positions considered.

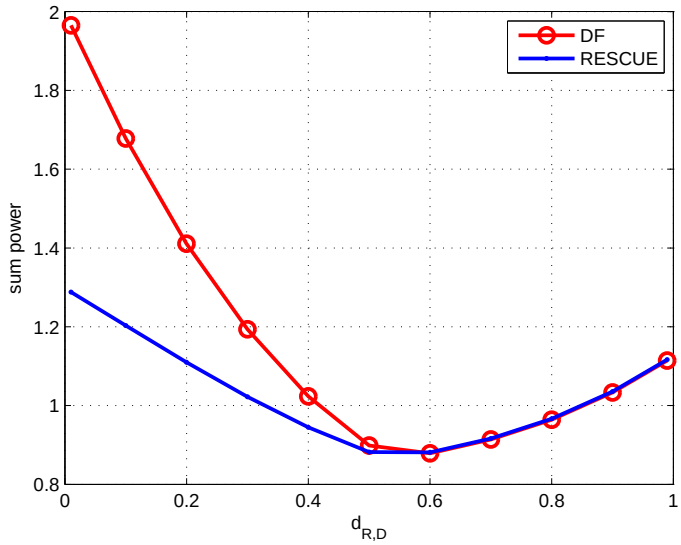

Figure 4.5: Sum power versus relay location.

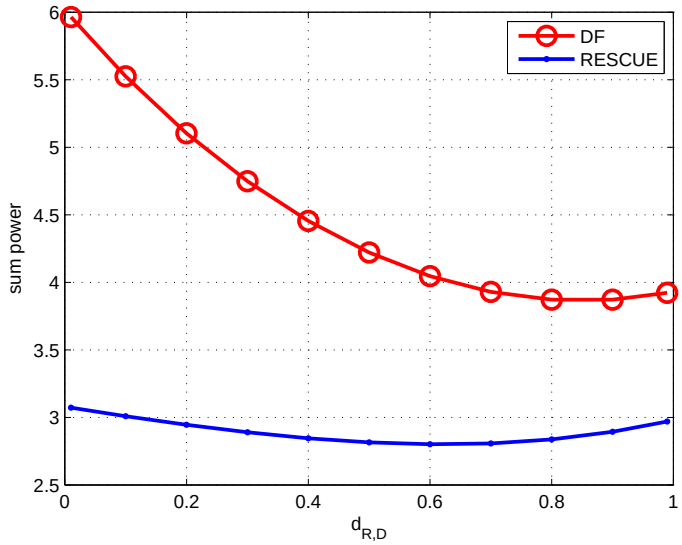

Figure 4.6: Sum power versus relay location.

4.6 Summary

Power allocation for TS4 with RESCUE functionality was investigated in this section. This work was about to provide the ultimate limits for the lossy MARC system and show how it performs compared to lossless DF. It was shown that the RESCUE scheme can achieve superior performance in terms of the total power consumption compared to the conventional DF strategy. It was shown that when the signal-to-noise power ratios of the links decrease, the performance gap between the lossy and lossless scheme increases. The RESCUE system presented in this section is especially beneficial in unpredictable environment, where the link budget is not enough to guarantee the lossless transmission.

5. Conclusion

In this deliverable, the intermediate results regarding the optimal power allocation and rate distortion minimization for different toy scenarios have been presented. With the concept of "links-on-the-fly", the objectives are mainly focusing on the outage probability minimization subject to the total power constraint and its dual of the transmit power minimization subject to the fixed outage probability constraint, where only statistic channel information are needed at the source/relay nodes for the power allocation. Apart from this, assuming the system with the local or global instantaneous channel information, some algorithms to solve the MIMO based sum-rate maximization problem and the power minimization problem under the lossy based rate region constraint have also been provided. Although the instantaneous channel information is difficult to obtain, such kind of analysis could be used as the baselines for the further power allocation research comparison.

In detail, the optimal power allocation algorithms for the basic erroneous DF relaying network (i.e., TS1) has been firstly investigated. Here, the optimal power allocation for the LosFoR based outage probability has been proposed, where the closed-form of the approximated outage probability has been provided, and its convexity has been proved. As shown in the simulation results, the approximation can ensure sufficient accuracy, and comparing with the equal power allocation, the proposed optimization can achieve much lower outage probability especially when the relay node is near to the destination node. Following, the system model has been extended to MIMO case in order to enjoy the increased multiplexing gain. In this case, for its simplicity, ZF based precoding/decoding matrices have been proposed for the interference cancellation. Then, the relay-oriented source power allocation algorithm for MIMO S-DF relaying has been developed to maximize the system sum-rate subject to the total source power constraint, and the simulation results have shown the improved system performance by comparing with the conventional relay assisted schemes.

The second consideration is the power allocation algorithms for solving the CEO problem. As the way of analysing the outage probability for TS1, the optimal power allocation algorithms to minimize the outage probability subject to the total power constraint and the total transmit power subject to the fixed outage probability for TS2 have also been investigated. As expected, comparing with the equal power allocation, the proposed algorithm has shown its improved performance in terms of the outage probability and energy saving. In addition, the distributed transmit power allocation among all relays for the CEO problem has also been investigated, which aims to equalize the SNR limits for each relay decoder. Such process can remove or reduce the ramp region of the joint decoder. The proposed algorithm has shown significant improvements in the SNR limits for the relay decoders, and the BER curve of the joint decoder qualitatively follows as expected.

Moreover, the optimal power allocation for orthogonal MARC allowing intra-link errors has also been investigated. In this case, in order to guarantee the reliable transmission of the lossy based system, the rate constraints have been provided, and the power optimization problem has been formulated as minimizing the total transmit power subject to simultaneously satisfy the provided lossy rate constraints. Such problem can be solved based on SCA algorithm, and convergence of the algorithm has been justified. It has been shown that the proposed scheme outperforms the conventional DF strategy in terms of the total power consumption. Furthermore, when SNRs of the links decrease, the performance gap between the lossy and lossless scheme increases.

To sum up, the intermediate results of optimal distributed power allocation algorithms have been provided, and the performances of proposed algorithms have been evaluated using the RESCUE provided toy scenarios which were presented in D1.2.1. For the next step, in order to further analyse the benefits of the "links-on-the-fly" concept, more comprehensive and practically used power allocation algorithms will be exploited through computer simulations and SDR platform test, and all of these will be documented in D2.2.2.

6. References

[AB14] H. Al-Tous and I. Barhumi. "Resource Allocation for Two-Users DF-OFDMA Systems". In: *Proc. IEEE Veh. Tech. Conf.* Sept. 2014, pp. 1–5. DOI: 10.1109/VTCFall.2014.6966158.

[AM12] K. Anwar and T. Matsumoto. "Accumulator-Assisted Distributed Turbo Codes for Relay Systems Exploiting Source-Relay Correlation". In: *IEEE Commun. Lett.* 16.7 (2012), pp. 1114–1117. ISSN: 1089-7798. DOI: 10.1109/LCOMM.2012.050112.120629.

[BCJ+74] L. R. Bahl, J. Cocke, F. Jelinek, and J. Raviv. "Optimal Decoding of Linear Codes for Minimizing Symbol Error Rate". In: *IEEE Trans. Inf. Theory* 20.2 (Mar. 1974), pp. 284–287.

[BK13] M. R. Bhatnagar and Arti M. K. "Selection Beamforming and Combining in Decode-and-Forward MIMO Relay Networks". In: *IEEE Commun. Lett.* 17.8 (Aug. 2013), pp. 1556–1559.

[BV04] S. Boyd and L. Vandenberghe. *Convex Optimization*. New York, NY: Cambridge University Press, 2004.

[BV10] S. Boyd and L. Vandenberghe. *Convex Optimization*. Vol. 25. Cambridge Univ. Pr., 2010, pp. 487–487. ISBN: 9780521833783. DOI: 10.1080/10556781003625177. arXiv: 1111.6189v1. URL: https://web.stanford.edu/~boyd/cvxbook/bv%5C_cvxbook.pdf.

[BZH96] T. Berger, Z. Zhang, and V. Harish. "The CEO-Problem". In: 42.3 (1996).

[CAM13a] M. Cheng, K. Anwar, and T. Matsumoto. "Outage based power allocation: Slepian-Wolf relaying viewpoint". In: *Proc. IEEE Global Telecommunications Workshops* (2013), pp. 807–811. DOI: 10.1109/GLOCOMW.2013.6825088.

[CAM13b] M. Cheng, K. Anwar, and T. Matsumoto. "Outage probability of a relay strategy allowing intra-link errors utilizing Slepian-Wolf theorem". In: *EURASIP Journal on Advances in Signal Process.* 2013.1 (2013), p. 34. ISSN: 1687-6180. DOI: 10.1186/1687-6180-2013-34.

[Cos83] M. Costa. "Writing on dirty paper (Corresp.)" In: *IEEE Trans. Inf. Theory* 29.3 (May 1983), pp. 439–441. DOI: 10.1109/TIT.1983.1056659.

[EZL+10] M. El Soussi, A. Zaidi, J. Louveaux, and L. Vandendorpe. "Sum-rate optimized power allocation for the OFDM multiple access relay channel". In: *Proc. IEEE Int. Conf. Acoustics, Speech and Signal Process.* Mar. 2010, pp. 1–6. DOI: 10.1109/ISCCSP.2010.5463433.

[GB15] Michael C Grant and Stephen P Boyd. *CVX Research*. 2015. URL: http://cvxr.com/cvx/.

[GG00] W. Gander and W. Gautschi. "ADAPTIVE QUADRATURE-REVISITED". In: *BIT* 40 (2000), pp. 84–101.

[GK11] A. E. Gamal and Y. H. Kim. *Network Information Theory*. Cambridge Univ. Press, 2011.

[Gol05] A. Goldsmith. *Wireless Communications*. New York, NY: Cambridge University Press, 2005.

[GZ05] J. Garcia-Frias and Y. Zhao. "Near-Shannon/Slepian-Wolf Performance for Unknown Correlated Sources Over AWGN Channels". In: *IEEE Trans. Commun.* 53.4 (Apr. 2005), pp. 555–559. ISSN: 0090-6778. DOI: 10.1109/TCOMM.2005.844959.

[LNH10] D. Liang, S. X. Ng, and L. Hanzo. "Relay-Induced Error Propagation Reduction for Decode-and-Forward Cooperative Communications". In: *Proc. IEEE Global Telecommun. Conf.* Dec. 2010, pp. 1–5. DOI: 10.1109/GLOCOM.2010.5683872.

[LTW04] J. N. Laneman, D. N. C. Tse, and G. W. Wornell. "Cooperative diversity in wireless networks: Efficient protocols and outage behavior". In: *IEEE Trans. Inf. Theory* 50.12 (Dec. 2004), pp. 3062–3080. DOI: 10.1109/TIT.2004.838089.

[LZA+14] P. Lu, X. Zhou, K. Anwar, and T. Matsumoto. "Joint Adaptive Network-Channel Coding for Energy-Efficient Multiple-Access Relaying". In: *IEEE Trans. Veh. Technol.* 63.5 (June 2014), pp. 2298–2305. ISSN: 0018-9545. DOI: 10.1109/TVT.2013.2292508.

[LZM14] P. Lu, X. Zhou, and T. Matsumoto. "Outage Probabilities of Orthogonal Multiple-Access Relaying Techniques with Imperfect Source-Relay Links". In: *IEEE Trans. Wireless Commun.* PP.99 (2014), pp. 1–1. ISSN: 1536-1276. DOI: 10.1109/TWC.2014.2384046.

[MW78] B. R. Marks and G. P. Wright. "Technical Note-A General Inner Approximation Algorithm for Nonconvex Mathematical Programs". In: *Operations Research* 26.4 (1978), pp. 681–683.

[NBK04] R. U. Nabar, H. Bolcskei, and F. W. Kneubuhler. “Fading Relay channel: performance limits and space-time signal design”. In: *IEEE J. Sel. Areas Commun.* 22.6 (Aug. 2004), pp. 1099–1109.

[NHH04] A. Nosratinia, T.E. Hunter, and A. Hedayat. “Cooperative communication in wireless networks”. In: *IEEE Commun. Mag.* 42.10 (Oct. 2004), pp. 74–80. ISSN: 0163-6804. DOI: 10.1109/MCOM.2004.1341264.

[SAK12] S. Schedler, A. Angierski, and V. Kuehn. “Resource allocation for the DF multiple access relay channel with OFDMA”. In: *Proc. Int. Symp. on Wireless Commun. Systems*. Aug. 2012, pp. 351–355. DOI: 10.1109/ISWCS.2012.6328388.

[Sha08] L. F. Shampine. “Matlab program for quadrature in 2D”. In: *Applied Mathematics and Computation* 202.1 (2008), pp. 266–274. ISSN: 0096-3003. DOI: http://dx.doi.org/10.1016/j.amc.2008.02.012. URL: http://www.sciencedirect.com/science/article/pii/S0096300308000982.

[Sha59] C. E. Shannon. “Coding theorems for a discrete source with a fidelity criterion”. In: *IRE Nat. Conv. Rec., Pt. 4*. 1959, pp. 142–163.

[Ver98] S. Verdu. *Multiuser Detection*. New York, NY: Cambridge University Press, 1998.

[VFC+14] F. J. Vazquez-Araujo, O. Fresnedo, L. Castedo, and J. Garcia-Frias. “Analog Joint Source-Channel Coding over MIMO channels”. In: *Eurasip J. on Wireless Commun. and Netw.* 2014:25 (2014).

[WMF15] A. Wolf, M. Matth, and G. Fettweis. “Improved Source Correlation Estimation in Wireless Sensor Networks”. In: *Proc. IEEE Int. Conf. Commun.* (2015), pp. 1–6.

[YG11] R. Youssef and A. Graell i Amat. “Distributed Serially Concatenated Codes for Multi-Source Cooperative Relay Networks”. In: *IEEE Trans. Wireless Commun.* 10.1 (Jan. 2011), pp. 253–263. ISSN: 1536-1276. DOI: 10.1109/TWC.2010.102810.100422.

[ZCH+14] X. Zhou, M. Cheng, X. He, and T. Matsumoto. “Exact and Approximated Outage Probability Analyses for Decode-and-Forward Relaying System Allowing Intra-Link Errors”. In: *IEEE Trans. Wireless Commun.* 13.12 (Dec. 2014), pp. 7062–7071. ISSN: 1536-1276. DOI: 10.1109/TWC.2014.2354337.

[ZMG+09] W. Zhang, X. Ma, B. Gestner, and D. V. Anderson. “Designing Low-complexity equalizers for wireless systems”. In: *IEEE Commun. Mag.* 47.1 (Jan. 2009), pp. 56–62.